NASA CONTRACTOR REPORT

NASA CR-1860

A SECOND ORDER SLENDER WING THEORY FOR WINGS WITH LEADING EDGE SEPARATION IN SUPERSONIC FLOW

by Joseph P. Nenni and Chee Tung

Prepared by
CORNELL AERONAUTICAL LABORATORY, INC.
Buffalo, N.Y. 14223
for Langley Research Center

NATIONAL AERONAUTICS AND SPACE ADMINISTRATION • WASHINGTON, D. C. • SEPTEMBER 1971

1. Report No.	2. Government Accession No.	3. Recipient's Catalog No.
NASA CR-1860		

4. Title and Subtitle

A SECOND-ORDER SLENDER WING THEORY FOR WINGS WITH LEADING-EDGE SEPARATION IN SUPERSONIC FLOW

5. Report Date
September 1971

6. Performing Organization Code

7. Author(s)

Joseph P. Nenni and Chee Tung

8. Performing Organization Report No.
AF-2883-S-1

9. Performing Organization Name and Address

Cornell Aeronautical Laboratory, Inc.
4455 Genesee Street
Buffalo, New York 14221

10. Work Unit No.
136-13-01-02

11. Contract or Grant No.
NAS1-9543

12. Sponsoring Agency Name and Address
National Aeronautics and Space Administration
Washington, D. C. 20546

13. Type of Report and Period Covered
Contractor Report

14. Sponsoring Agency Code

15. Supplementary Notes

16. Abstract

A second-order slender wing theory has been developed for calculating the supersonic flow over low aspect ratio wings with subsonic leading edges and leading-edge separation. The theory is second order in terms of the ratio of span to chord. The theory has been developed by using a combined application of the method of strained coordinates and matched asymptotic expansions. The Brown and Michael flow model has been used to model the leading-edge separation. The theory is compared with experiment for delta wings and provides a substantial improvement over previous slender wing results but still overestimates normal force. The theory qualitatively predicts the correct Mach number trend and approaches the correct level for a sonic leading edge. The trend is somewhat overpredicted, however, producing best agreement at the higher Mach numbers.

17. Key Words (Suggested by Author(s))	18. Distribution Statement
Low Aspect Ratio Wings Mathematical Method of Matched Asymptotic Expansions Mathematical Method of Strained Coordinates Delta Wings Brown and Michael Flow Model	Unclassified - Unlimited

19. Security Classif. (of this report)	20. Security Classif. (of this page)	21. No. of Pages	22. Price*
Unclassified	Unclassified	66	$3.00

*For sale by the National Technical Information Service, Springfield, Virginia 22151

TABLE OF CONTENTS

I. SUMMARY

A second order slender wing theory has been developed for calculating the supersonic flow over low aspect ratio wings with subsonic leading edges and leading edge separation. The theory is second order in terms of the ratio of span to chord. The theory has been developed by using a combined application of the method of strained coordinates and matched asymptotic expansions. The Brown and Michael flow model has been used to model the leading edge separation. The theory is compared with experiment for delta wings and provides a substantial improvement over previous slender wing results but still overestimates normal force. The theory qualitatively predicts the correct Mach number trend and approaches the correct levels for a sonic leading edge. The trend is somewhat overpredicted, however, producing best agreement at the higher Mach numbers.

II. LIST OF SYMBOLS

a	ratio of span to root chord, $\frac{b}{c}$
A	aspect ratio
A_1	function defined by Equation (C-3)
b	half span of wing at trailing edge
B	source strength defined by Equation (B-17a)
c	half root chord of wing
C_L	lift coefficient
C_N	normal force coefficient
C_p	pressure coefficient
ΔC_p	difference between upper and lower surface pressure coefficients
d	radius of cylinder in ζ plane (see Figure 15B)
$E(k)$	complete elliptic integral of second kind of modulus k
f_i, f_i	gage functions used in Equations (A-1) and (A-3)
F_1	complex function defined by Equation (58)
$\bar{G}_2$	normal force function defined by Equation (B-14)
$h(x)$	normalized half span of wing as a function of x
H_1	function defined by Equation (45)
H_5	function defined by Equation (44)
H_6	function defined by Equation (C-8)
i	$\sqrt{-1}$

$I.P.$	designates imaginary part of complex quantity
k	modulus of elliptic integral or edge angle parameter for biconvex profile (see Figure 15A)
K	function of Mach number $\left(K = M^2\left[2 - M^2(1-\gamma)\right]\right)$
$\bar{K}$	function of Mach number $\left(\bar{K} = \frac{K}{2\beta^2}\right)$
$L(\psi_i)$	operational notation for wave operator (see Equation (7))
M	freestream Mach number
p	real coordinate of vortex core in physical plane
$\tilde{p}$	normalized real coordinate of vortex core $(\tilde{p} = p/k)$
$\bar{P}(s)$	doublet strength for outer solution
q	imaginary coordinate of vortex core in physical plane or sound speed
$\tilde{q}$	normalized imaginary coordinate of vortex core $(\tilde{q} = q/k)$
r	distance from S axis in S, η, ζ space $(r = \sqrt{\eta^2 + \zeta^2})$
R_1	function defined by Equation (C-4)
R_2	function defined by Equation (C-5)
$R.P.$	designates real part of complex quantity
s	surface shape function
S, η, ζ	strained outer variables (defined by Equation (6))
S, Y, Z	strained inner variables defined by Equation (24)
$\bar{t}$	wing thickness ratio in cross flow plane

T	surface thickness function
u	normalized span coordinate ($u = z/h$)
u, v, w	cartesian velocity component in x, y, z direction respectively
W_{11}	complex potential for first inner solution for infinitely thin wing
W_{121}	complex function whose real part is Φ_{121}
W_{41}	complex function whose real part is Φ_{41}
$\mathcal{W}_{11}$	complex potential for first inner solution for biconvex profile wing
x, y, z	cartesian coordinates normalized by c
α	angle of attack
α_1	angle defined by Equation (C-13)
α_2	angle defined by Equation (C-15)
β	$\sqrt{M^2-1}$
β_1	angle defined by Equation (C-6)
β_2	angle defined by Equation (C-7)
γ	ratio of specific heats
Γ	vortex strength
ϵ	small parameter or thickness ratio
$\bar{\epsilon}$	angle of attack parameter ($\bar{\epsilon} = \frac{\sin\alpha}{\tan\Lambda}$)
ζ	transformed complex variable defined by Equation (B-5)
$\zeta_1, \bar{\zeta}_1$	Vortex position and conjugate position in ζ plane

θ	edge angle for biconvex profiles (see Figure 15A)
θ_1	angle defined by Equations (C-12) and (C-14)
θ_2	angle defined by Equation (C-16)
θ_4	angle defined by Equation (B-17b)
λ	real vortex coordinate in χ plane
$\tilde{\lambda}$	normalized real vortex coordinate ($\tilde{\lambda} = \frac{\lambda}{b}$)
ξ	outer complex variable ($\xi = a\sigma$)
ξ_1 , ξ_2	straining of χ coordinate
σ	complex inner variable
σ_1 , $\bar{\sigma}_1$	vortex position and conjugate position in σ plane
Λ	delta wing semi-apex angle
τ	imaginary vortex coordinate in χ plane
$\tilde{\tau}$	normalized imaginary vortex coordinate ($\tilde{\tau} = \frac{\tau}{b}$)
$\bar{\phi}$	velocity potential
$\dot{\Phi}^{\lambda}_{11}$, $\dot{\Phi}^{\lambda}_{121}$, $\dot{\Phi}^{\lambda}_{122}$ $\dot{\Phi}^{\lambda}_{41}$	inner solutions for velocity potential
χ	complex transform of σ plane (see Figure 19)
ψ_1 , ψ_2	decomposition of $\bar{\phi}$ (see Equation (5))

III. INTRODUCTION

The nonlinear aerodynamic characteristics of low aspect ratio or slender wings have been the subject of extensive theoretical and experimental investigations over the past several years. The prime motivation of these investigations has been the application to the low speed and supersonic aerodynamic problems of high-speed aircraft and lifting reentry vehicles. Moreover, a further understanding of the flow over such wings would also aid in the design of optimum wings for supersonic flight.

The unique feature of the flow fields over slender wings is the leading edge separation. Spiral vortex sheets emanate from the leading edges and dominate the upper wing surface flow field. (Such a flow is shown schematically in Figure 1.) Because the vortex lines on these sheets are very highly swept with respect to the freestream the areas of significant total pressure loss are confined only to the core area of the spiral sheet and to a small area adjacent to the leading edge. Therefore, an inviscid flow analysis should be capable of treating the major details of the flow field.

Although an accurate analytical method utilizing an intuitive leading-edge suction analogy exists for estimating overall forces on slender wings, Reference 1, methods to predict detailed flow field quantities and surface pressure distributions are needed.

From a mathematical viewpoint the separated flow results in a nonlinearity through the boundary conditions because the location of the vortex sheets is not known a priori. The existing analyses of low aspect ratio wings have employed the slender wing or slender body approximations whereby the problem can be reduced to a quasi two-dimensional problem in the cross flow plane. The cross flow problem is still nonlinear through the boundary conditions, but in the two-dimensional case the problem may be solved with complex variable theory. The existing analyses, References 2 through 4, differ only in their representation of the spiral vortex sheet. The simplest representation is that of Brown and Michael (Reference 2). The sheet representation that physically corresponds closest to experimental observation is that of Smith (Reference 4). All of these theories, however, considerably overestimate the forces on slender wings.

Most correlations of theory and experiment have been made with slender delta wings. Although the slender wing theory results are independent of Mach number, the delta wing solutions are conical and therefore only appropriate at supersonic speeds. At subsonic speeds the conical solutions violate the Kutta conditions at the trailing edge and hence the correlation is expected to be poor.

If it is assumed that Reference 4 presents an adequate model of the cross flow then the reasons for the failure of these theories in the supersonic flow case is evidently due to the slenderness assumptions employed and/or neglect of the nonlinear terms in the equations of motion. The present work corrects these deficiencies by developing corrections to the slender wing theory for non-slenderness and nonlinearity in the equations of motion. This is done by developing a formal systematic expansion procedure for the velocity potential in which slender wing theory is the first term in the expansion. This approach retains the simplicity and advantages of the cross flow approach of slender wing theory and has had some success in the incompressible flow case. Reference 5. The terminology of perturbation theory as defined in Reference 6 is used throughout this report.

The slender wing problem involves several small parameters in which an expansion may be considered (for example, angle of attack, thickness ratio, and aspect ratio). The problem then is to devise an expansion procedure that accounts properly for all of these small parameters.

For supersonic flow the problems associated with a straightforward perturbation scheme in terms of angle of attack and/or thickness are fairly well known. (See, for example, Reference 6.) The first terms in such a scheme are the well-known linear theory of supersonic flow. Problems, however, arise with the higher order terms. In two-dimensional flow, the second order terms become unbounded far from the body as may be shown from the results of Reference 7. In three-dimensional flow the second order terms compound the order of singularities of the first-order solution to the point that the pressure distributions are generally non-integrable. The method of strained coordinates, Reference 8, has been developed to remedy these types of nonuniformities. A more heuristic argument of the physical reasons for the failures of a straightforward perturbation scheme may be found in Reference 9.

The strained coordinate technique is well developed for two-dimensional problems (see Chapter 6, Reference 6), but is not well developed for three-dimensional wing problems. The difficulty with application to wings lies in the analytical evaluation of the particular integrals required for the higher order solutions. Clarkson, Reference 10, has formulated the general three-dimensional problem and presents a solution for a rolling wing with straight, unswept trailing and leading edges. No solutions exact to second-order are known for wings of more practical interest.

Sugo, Reference 11, has obtained approximate expressions for the particular integrals required for the case of a delta wing with subsonic and supersonic leading edges. (The spiral vortex sheets are not modeled for the subsonic leading edge case.) The approximation, however, does not correspond to a formal systematic expansion procedure. This has prompted Lee, Reference 12, to propose a slightly different approximate particular integral for the supersonic leading edge case. Lee's work also does not correspond to a formal systematic approximation procedure so that both works are somewhat arbitrary from this standpoint. In both works the straining is chosen to control the growth of singularity in the higher order solutions without regard for the far field nonuniformities of the higher order solutions.

The present work overcomes these limitations by using the technique of matched asymptotic expansions to obtain a formal systematic approximation for the required particular integrals and to develop a straining that simultaneously controls the singularities and far field nonuniformities of the second order solution. Although the techniques of strained coordinates and matched asymptotic expansions are well documented in the literature, a short outline of these two methods which is sufficient for their application to the present problem is contained in Appendix A.

The Brown and Michael cross flow model, Reference 2, was used for the cross flow model of the present work. This selection was made in order to facilitate evaluation of the overall expansion scheme. This selection allows almost complete analytical solution to the problem. Although the flow model of Smith, Reference 4, would appear to be more physically realistic, the overall forces predicted by this model are only slightly different from those

of Reference 2. Hence, the additional complexities of the Smith model are not warranted until the overall expansion scheme is evaluated.

The major portion of this report presents the formulation of the general three-dimensional problem, including thickness, and the second order solution for the infinitely thin flat wing.

All of the existing slender wing treatments are for infinitely thin wings. The effect of thickness upon the flow field is then an open question from the theoretical viewpoint, at least. For those conditions where the vortex sheet lies close to the wing the thickness of the wing may be significant. This has prompted the consideration of wing thickness. A slender wing analysis employing the ideas of the Brown and Michael flow model has been completed for a conical wing with biconvex circular arc profile in the cross flow plane. Although the complete second order solution has not been obtained, no other analysis accounting for thickness is available and it was therefore considered appropriate to present the slender wing analysis in Appendix B.

IV. FORMULATION OF GENERAL PROBLEM

The overall expansion scheme employed first assumes an expansion of the velocity potential in terms of thickness and angle of attack. This decomposes the solution into a sequence of linear problems. These linear problems are then solved by the matched asymptotic expansion technique using α, the ratio of span to root chord, as the small parameter.

The fluid is assumed to be perfect, and the flow is assumed to be irrotational. Then a velocity potential $\bar{\Phi}$ exists such that

$$u = \bar{\Phi}_x \quad ; \quad v = \bar{\Phi}_y \quad ; \quad w = \bar{\Phi}_z \tag{1}$$

(the coordinate system used is shown in Figure 2).

The momentum equation may then be expressed as (Reference 13)

$$(q^2 - \bar{\Phi}_x^2)\,\bar{\Phi}_{xx} + (q^2 - \bar{\Phi}_y^2)\,\bar{\Phi}_{yy} + (q^2 - \bar{\Phi}_z^2)\,\bar{\Phi}_{zz} - 2\,\bar{\Phi}_x \bar{\Phi}_y \bar{\Phi}_{xy} - 2\,\bar{\Phi}_x \bar{\Phi}_z \bar{\Phi}_{zx} - 2\,\bar{\Phi}_y \bar{\Phi}_z \bar{\Phi}_{zy} = 0 \tag{2}$$

and the energy equation may be expressed as

$$q^2 = q_\infty^2 + \frac{\gamma - 1}{2} U_\infty^2 - \frac{\gamma - 1}{2} (\bar{\Phi}_x^2 + \bar{\Phi}_y^2 + \bar{\Phi}_z^2) \tag{3}$$

where q is the local speed of sound and a subscript of ∞ refers to the free-stream conditions ahead of the wing. The subscript notation is used for differentiation. A body axis system is used and the wing surface ordinates are given in the form $\mathcal{S}(x, y, z) = 0$. The boundary condition of flow tangency at the wing surface is then given by

$$\nabla \bar{\Phi} \cdot \nabla \mathcal{S} = 0 \qquad \text{on} \qquad \mathcal{S} = 0 \tag{4}$$

where ∇ is the vector differential operator $\nabla \equiv \bar{i} \frac{\partial}{\partial x} + \bar{j} \frac{\partial}{\partial y} + \bar{k} \frac{\partial}{\partial z}$ and the dot signifies the dot product.

The interest is in thin wings of small aspect ratio at small angles of attack. In the body axis system, then, the wing surface is expressible in the form

$$F(y,z) = \epsilon T(x)$$

where ϵ is a small parameter that serves as a measure of the wing thickness. For wings of small thickness at small incidences an expansion of the velocity potential $\bar{\Phi}$ of the form

$$\bar{\Phi} \sim U_\infty \left\{ x \cos\alpha + \sin\alpha\, \psi_1 + \epsilon\, \psi_2 + \epsilon \sin\alpha\, \psi_3 + \sin^2\alpha\, \psi_4 + \epsilon^2\, \psi_5 + o(\epsilon^3, \epsilon^2 \sin\alpha, \epsilon \sin^2\alpha, \sin^3\alpha) \right\} \tag{5}$$

is assumed. The independent spatial variables x, y, z are also expanded in the form

$$y = \eta \tag{6a}$$
$$z = \zeta \tag{6b}$$
$$x = S + \xi_1 \sin\alpha + \epsilon\, \xi_2 \tag{6c}$$

Here ξ_1 and ξ_2 are the straining required to keep the first order solution uniformly valid in the entire flow field. The original nonlinear problem may now be decomposed into a sequence of linear problems by substituting Equations (5) and (6) into Equations (2) and (3) and equating like powers of the gage functions, ϵ and $\sin\alpha$. This procedure produces the following sequence of partial differential equations for the ψ_i

for $i = 1$

$$L(\psi_1) \equiv \psi_{1SS}(1 - M^2) + \psi_{1\eta\eta} + \psi_{1\zeta\zeta} = 0 \tag{7}$$

for $i = 2$

$$L(\psi_2) \equiv \psi_{2SS}(1 - M^2) + \psi_{2\eta\eta} + \psi_{2\zeta\zeta} = 0 \tag{8}$$

for $i = 3$

$$L(\psi_3) = (\psi_{1_s}\,\psi_{2_{sss}} + \psi_{2_s}\,\psi_{1_{sss}})\left\{M^2(\gamma+1) + M(\gamma-1)(M^2-1)\right\} \tag{9}$$

$$+ 2(1-M^2)\left\{\xi_{2_s}\,\psi_{1_{ss}} + \xi_{1_s}\,\psi_{2_{ss}}\right\} + 2M^2(\psi_{2_\xi}\,\psi_{1_\xi} + \psi_{2_\eta}\,\psi_{1_\eta})_s$$

$$+ 2(\xi_{2_\eta}\,\psi_{1_{s_\eta}} + \xi_{1_\eta}\,\psi_{2_{s_\eta}} + \xi_{1_\xi}\,\psi_{2_{s_\xi}} + \xi_{2_\xi}\,\psi_{1_{s_\xi}})$$

for $i = 4$

$$L(\psi_4) = \psi_{1_s}\,\psi_{1_{ss}}\left\{M^2(\gamma+1) + M^2(\gamma-1)(M^2-1)\right\} \tag{10}$$

$$+ 2(1-M^2)\,\xi_{1_s}\,\psi_{1_{ss}} + 2\,\xi_{1_\eta}\,\psi_{1_{\eta_s}} + 2\,\xi_{1_\xi}\,\psi_{1_{\xi_s}} + M^2(\psi_{1_\eta}^2 + \psi_{1_\xi}^2)_s$$

for $i = 5$

$$L(\psi_5) = \psi_{2_s}\,\psi_{2_{ss}}\left\{M^2(\gamma+1) + M^2(\gamma-1)(M^2-1)\right\} \tag{11}$$

$$+ 2(1-M^2)\,\xi_{2_s}\,\psi_{2_{ss}} + M^2(\psi_{2_\eta}^2 + \psi_{2_\xi}^2)_s$$

The corresponding boundary conditions are found by an application of the same procedure to Equation (4). It is first noted that for the class of wings under consideration that

$$\mathcal{J}_\eta \sim O(1)$$

$$\mathcal{J}_\xi \sim O(1)$$

$$\mathcal{J}_s = \epsilon\,\bar{\mathcal{J}}_s$$

where

$$\bar{\mathcal{J}}_s \sim O(1)$$

then

for $i = 1$

$$\mathcal{J}_\eta \psi_{1\eta} + \mathcal{J}_\zeta \psi_{1\zeta} = 0 \quad on \quad \mathcal{J} = 0 \tag{12}$$

for $i = 2$

$$\bar{\mathcal{J}}_s \cos\alpha + \mathcal{J}_\eta \psi_2 + \mathcal{J}_\zeta \psi_{2\zeta} = 0 \quad on \quad \mathcal{J} = 0 \tag{13}$$

for $i = 3$

$$\mathcal{J}_\eta \psi_{3\eta} + \mathcal{J}_\zeta \psi_{3\zeta} = \cos\alpha \xi_{1s} \bar{\mathcal{J}}_s + \mathcal{J}_\eta (\psi_{1s} \xi_{2\eta} + \psi_{2s} \xi_{1\eta}) \tag{14}$$

$$+ \mathcal{J}_\zeta (\xi_{2\zeta} \psi_{1s} + \xi_{1\zeta} \psi_{2s}) \quad on \quad \mathcal{J} = 0$$

for $i = 4$

$$\mathcal{J}_\eta \psi_{4\eta} + \mathcal{J}_\zeta \psi_{4\zeta} = \psi_{1s} (\mathcal{J}_\zeta \xi_{1\zeta} + \mathcal{J}_\eta \xi_{1\eta}) \quad on \quad \mathcal{J} = 0 \tag{15}$$

for $i = 5$

$$\mathcal{J}_\eta \psi_{5\eta} + \mathcal{J}_\zeta \psi_{5\zeta} = \bar{\mathcal{J}}_s (\cos\alpha \xi_{2s} - \psi_{2s}) \tag{16}$$

$$+ \psi_{2s} (\xi_{2\eta} \mathcal{J}_\eta + \xi_{2\zeta} \mathcal{J}_\zeta) \quad on \quad \mathcal{J} = 0$$

Here it will be noted that all the conditions are applied on the body itself, $\mathcal{J} = 0$. It would be permissible to transfer the boundary conditions to the $\eta = 0$ plane via a Taylor series expansion of Equations (12) through (16) about the $\eta = 0$ plane. This procedure has not been followed here because it proves more expedient for the present analysis to satisfy the boundary conditions on the body itself.

At this stage it will be noted that Equations (7) and (12) constitute the

standard lifting problem from linear theory, and Equations (8) and (13) constitute the standard thickness problem from linear theory. The ψ_3, ψ_4 and ψ_5 terms are corrections to the linear theory to account for the nonlinear terms in the equations of motion neglected in the first approximation.

The small angle expansion of $\cos\alpha$ is required to obtain Equations (8), (9) and (10). If this expansion is not used, an incompatible set of equations for the higher order solutions is developed.

In isentropic flow the pressure coefficient C_p may be obtained from the energy equation as

$$C_p = \frac{2}{\gamma M^2}\left\{\left[1 + \frac{\gamma-1}{2}M^2\left(1 - \frac{\bar\phi_x^2 + \bar\phi_y^2 + \bar\phi_z^2}{U_\infty^2}\right)\right]^{\frac{\gamma}{\gamma-1}} - 1\right\} \tag{17}$$

In terms of the ψ_i, and retaining terms through second-order in the gage functions, this becomes:

$$\begin{aligned} C_p \approx\ & -2\sin\alpha\cos\alpha\,\psi_{1_s} - 2\epsilon\cos\alpha\,\psi_{2_s} + \epsilon\sin\alpha\left\{M^2\psi_{1_s}\psi_{2_s}\right. \\ & \left. - 2\cos\alpha\,(\psi_{3_s} - \psi_{1_s}\xi_{2_s} - \psi_{2_s}\xi_{1_s}) - 2(\psi_{1_s}\psi_{2_s} + \psi_{1_\eta}\psi_{2_\eta} + \psi_{1_\zeta}\psi_{2_\zeta})\right\} \\ & + \sin^2\alpha\left\{M^2\psi_{1_s}^2 - 2\cos\alpha\,(\psi_{4_s} - \psi_{1_s}\xi_{1_s}) - (\psi_{1_s}^2 + \psi_{1_\eta}^2 + \psi_{1_\zeta}^2 - 1)\right\} \\ & + \epsilon^2\left\{M^2\psi_{2_s}^2 - 2\cos\alpha\,(\psi_{5_s} - \psi_{2_s}\xi_{2_s}) - (\psi_{2_s}^2 + \psi_{2_\eta}^2 + \psi_{2_\zeta}^2)\right\} \end{aligned} \tag{18}$$

The ψ_i are now determined by the method of matched asymptotic expansions using the ratio of span to chord, a, as the small parameter for expansion purposes (sometimes referred to as slenderness parameter).

Thus, the overall expansion scheme may be summarized as first an expansion of the velocity potential in terms of $\sin\alpha$, and ϵ, with a subsequent expansion in terms of a, the slenderness parameter. The order of expansion with respect to these parameters is found to be crucial. The initial expansion must be made in terms of $\sin\alpha$ in order to avoid an anomalous dependence on the axis system employed.

V. INFINITELY THIN FLAT WING

For an infinitely thin wing $\epsilon = 0$. The velocity potential, Equation (5), is reduced to

$$\bar{\phi} \sim U_\infty \left\{ x \cos\alpha + \sin\alpha\, \psi_1 + \sin^2\alpha\, \psi_4 + o(\sin^3\alpha) \right\} \qquad (19)$$

and the corresponding independent variables expand as

$$y = \eta \qquad (20a)$$
$$z = \zeta \qquad (20b)$$
$$x = s + \xi_1 \sin\alpha \qquad (20c)$$

The wing planform is given by $z_{l.e} = a\, h(x)$; $0 \le h(x) \le 1$

Solution for ψ_1

The partial differential equation for ψ_1 is Equation (7). The boundary condition, Equation (12), becomes

$$\psi_{1_\eta} = 0 \quad \text{on} \quad \eta = 0 \; ; \quad |\zeta| \le a h \qquad (21)$$

ψ_1 is then determined by the method of matched asymptotic expansions. The outer expansion of ψ_1 valid far from the wing and valid for small a is of the form

$$\psi_1^\circ \sim \eta + a^2 \phi_{11}^\circ + a^4 \phi_{12}^\circ + \cdots \qquad (22)$$

where

$$\phi_{ij}^\circ = \phi_{ij}^\circ(\eta, \zeta, s)$$

ϕ_{11}° satisfies the wave equation, and in the limit as $a \to 0$ the wing shrinks to a line which may be represented by a line doublet distribution. Such a

potential is

$$\phi_{11}^{\circ} = \frac{1}{4\pi} \frac{\eta}{\eta^2 + \zeta^2} \int_{-1}^{S-\beta r} \frac{\bar{P}(S_o)\,(S - S_o)}{[(S - S_o)^2 - \beta^2 r^2]^{1/2}}\, d S_o \qquad (23)$$

where $r^2 = \eta^2 + \zeta^2$ and $\beta = \sqrt{M^2 - 1}$

The doublet strength is $\bar{P}(S_o)$ and is presently unknown. It will be determined by matching with an inner solution.

The inner problem is obtained by stretching the coordinates normal to the wing to regain the detail lost near the wing. The inner variables are

$$Y = \eta/a \qquad (24a)$$

$$Z = \zeta/a \qquad (24b)$$

$$S = S \qquad (24c)$$

The inner solution valid near the wing for small values of a is of the form

$$\psi_1^{i} \sim a\, \bar{\Phi}_{11}^{i}(Y, Z; S) + a^3\, \bar{\Phi}_{121}^{i}(Y, Z; S) + a^3 \ln a\, \bar{\Phi}_{122}^{i}(Y, Z; S) \qquad (25)$$

Substitution of Equations (24) and (25) into Equation (7) and equating like powers of a further decomposes the problem into the following sequence of problems.

for $\bar{\Phi}_{11}^{i}$: $\bar{\Phi}_{11_{YY}}^{i} + \bar{\Phi}_{11_{ZZ}}^{i} = 0$ (26)

for $\bar{\Phi}_{121}^{i}$: $\bar{\Phi}_{121_{YY}}^{i} + \bar{\Phi}_{121_{ZZ}}^{i} = \beta^2 \bar{\Phi}_{11_{SS}}^{i}$ (27)

for $\bar{\Phi}_{122}^{i}$: $\bar{\Phi}_{122_{YY}}^{i} + \bar{\Phi}_{122_{ZZ}}^{i} = 0$ (28)

with boundary conditions:

$$\bar{\Phi}_{11}^{i} \sim Y \quad \text{for} \quad Z, Y \longrightarrow \infty \qquad (29a)$$

$$\dot{\Phi}^{i}_{11_Y} = 0 \quad \text{for} \quad Y = 0, \quad |Z| \leq h(s) \tag{29b}$$

$$\dot{\Phi}^{i}_{121_Y} = 0 \quad \text{for} \quad Y = 0, \quad |Z| \leq h(s) \tag{30}$$

$$\dot{\Phi}^{i}_{122_Y} = 0 \quad \text{for} \quad Y = 0, \quad |Z| \leq h(s) \tag{31}$$

Equations (26) and (29) are recognized as the familiar cross flow problem from slender wing theory (Reference 14).

For the present problem the flow model of Brown and Michael (Reference 2) has been used. This cross flow model is shown in Figure 3. The model consists of the horizontal slit which represents the trace of the wing in the cross flow plane plus two concentrated vortices located symmetrically about the vertical axis on the lee side of the wing. The strengths of the vortices are of equal magnitude but opposite sense. The vortices of strength Γ are located at σ_1 and $-\bar{\sigma}_1$ in the complex plane. The appropriate $\dot{\Phi}^{i}_{11}$ may then be expressed as

$$\dot{\Phi}^{i}_{11} = R.P. \; W_{11}(\sigma; s) \tag{32}$$

where σ is the complex variable $Z + iY$ in the cross flow plane and

$$W_{11} = -i\left\{\sqrt{\sigma^2 - h^2} + \frac{\Gamma}{2\pi}\left[\ln\left(\sqrt{\sigma^2 - h^2} - \sqrt{\sigma_1^2 - h^2}\right) - \ln\left(\sqrt{\sigma^2 - h^2} + \sqrt{\bar{\sigma}_1^2 - h^2}\right)\right]\right\} \tag{33}$$

For conical flow the method of determining Γ and σ_1 may be found in Appendix B.

The two term outer expansion of Equation (33) is

$$a\,\dot{\Phi}^{i}_{11} \sim R.P.\; i\left\{\xi\left(1 - \frac{1}{2}\frac{a^2h^2}{\xi^2}\right) - \frac{\Gamma}{2\pi}\frac{a^2}{\xi^2}\left(\sqrt{\sigma_1^2 - h^2} + \sqrt{\bar{\sigma}_1^2 - h^2}\right)\right\} \tag{34}$$

where $\xi = a\sigma$.

In terms of the inner variables this is

$$a\dot{\Phi}^{i}_{11} \sim aY + \frac{aY}{Y^2 + Z^2}\left(\frac{h^2}{2} + \frac{\Gamma\lambda}{\pi}\right) \tag{35}$$

where the substitution

$$\sqrt{\sigma_1^2 - h^2} = \lambda + i\tau = h(\tilde{\lambda} + i\tilde{\tau}) \tag{36a}$$

$$\sqrt{\bar{\sigma}_1^2 - k^2} = \lambda - i\tau = k(\tilde{\lambda} - i\tilde{\tau}) \tag{36b}$$

has been used.

The one term inner expansion of Equation (23) is

$$a^2\phi_{11}^{\circ} \sim \frac{aY}{Y^2+Z^2}\,\frac{1}{4\pi}\int_{-1}^{S}\bar{P}(s_0)\,ds_0 \tag{37}$$

Application of the asymptotic matching principle yields

$$\bar{P}(S) = 4\pi\left(\frac{k^2}{2} + \frac{\Gamma\lambda}{\pi}\right)' \tag{38}$$

where the prime indicates differentiation with respect to S . For the case of no leading edge separation, ($\Gamma = 0$) Equation (38) leads directly to the well known slender wing result

$$C_N = \frac{\pi A}{2}\sin\alpha\cos\alpha$$

The next term in the inner solution may now be determined. The inhomogeneous equation for Φ_{121}^{i} , Equation (27), is solved by first transforming the independent variables by

$$\sigma = Z + iY \tag{39a}$$

$$\bar{\sigma} = Z - iY \tag{39b}$$

Then let $\Phi_{121}^{i} = R.P.\ W_{121}$. Equation (27) then becomes

$$4\,\frac{\partial^2 W_{121}}{\partial\sigma\,\partial\bar{\sigma}} = \beta^2\,\frac{\partial^2 W_{11}}{\partial S^2}\,. \tag{40}$$

W_{121} is then composed of a particular solution that satisfies Equation (40) plus a complementary solution that satisfies the corresponding homogeneous

equation, i.e. $W_{121} = W_{121}(P) + W_{121}(C)$. $W_{121}(P)$ is determined immediately by integration of Equation (40) as

$$W_{121}(P) = -i \frac{\beta}{4} \frac{\partial^2}{\partial S^2} \left\{ \bar{\sigma} \left(\frac{\sigma}{2} \sqrt{\sigma^2 - h^2} - \frac{h^2}{2} \cosh^{-1} \frac{\sigma}{h} \right) \right.$$

$$+ \frac{\Gamma}{2\pi} \bar{\sigma} \left(\sigma \ln \frac{\sqrt{\sigma^2 - h^2} - \sqrt{\sigma_1^2 - h^2}}{\sqrt{\sigma^2 - h^2} + \sqrt{\sigma_1^2 - h^2}} + \sigma_1 \ln 2 \left[\frac{\sigma\sigma_1 + h^2 + \sqrt{\sigma_1^2 - h^2}\sqrt{\sigma^2 - h^2}}{\sqrt{\sigma^2 - h^2} - \sqrt{\sigma_1^2 - h^2}} \right] \right.$$

$$- \bar{\sigma}_1 \ln 2 \left[\frac{\sigma\bar{\sigma}_1 + h^2 - \sqrt{\bar{\sigma}_1^2 - h^2}\sqrt{\sigma^2 - h^2}}{\sqrt{\sigma^2 - h^2} + \sqrt{\bar{\sigma}_1^2 - h^2}} \right] - \sqrt{\sigma_1^2 - h^2} \ln \frac{2}{h} \left[\sigma + \sqrt{\sigma^2 - h^2} \right]$$

$$\left. \left. - \sqrt{\bar{\sigma}_1^2 - h^2} \ln \frac{2}{h} \left[\sigma + \sqrt{\sigma^2 - h^2} \right] \right) \right\} \qquad (41)$$

Except for a multiplicative constant and constant of integration, this solution is the same as the particular solution for the incompressible case (Reference 5). The complementary portion of the solution is determined so as to meet the boundary condition, Equation (30), and to match with the inner expansion of the outer solution. The required expansion of the outer solution is the two term inner expansion of Equation (22) which is

$$\psi_1^{\circ} \sim a \left(Y + \frac{Y}{4\pi (Y^2 + Z^2)} \int_{-1}^{S} \bar{P}(S_0)\, dS_0 \right)$$

$$- a^3 \beta^2 \frac{Y}{4\pi} \left\{ \bar{P}'(S) \left(\frac{1}{4} + \frac{1}{2} \ln \frac{2}{\beta} \right) + \frac{1}{2} \left(\frac{\bar{P}(-1)}{1+S} + \bar{P}'(-1) \ln (1+S) \right) \right.$$

$$+ \bar{P}''(-1) \left[(1+S) \ln (1+S) - (1+S) \right] + \int_{-1}^{S} \bar{P}'''(S_0) \left[(S - S_0) \ln (S - S_0) \right.$$

$$\left. \left. - (S - S_0) \right] dS_0 \right) + \bar{P}'(S) \ln \sqrt{Y^2 + Z^2} \left. \right\} + a^3 \beta^2 \ln a \frac{Y \bar{P}'(S)}{8\pi} \qquad (42)$$

The complete second inner solution which satisfies the boundary condition Equation (30), and whose outer expansion matches Equation (42) is found by inspection to be

$$W_{121} = -\frac{\beta^2}{4} i \frac{\partial^2}{\partial s^2} \left\{ (\bar{\sigma} - \sigma)\left(\frac{\sigma}{2} \sqrt{\sigma^2 - h^2} - \frac{h}{2} \cosh^{-1} \frac{\sigma}{h} \right) \right.$$

$$+ \frac{\Gamma}{2\pi} (\bar{\sigma} - \sigma) \left[\ln 2 \left(\frac{\sqrt{\sigma^2 - h^2} - \sqrt{\sigma_1^2 - h^2}}{\sqrt{\sigma^2 - h^2} + \sqrt{\bar{\sigma}_1^2 - h^2}} \right) + \sigma_1 \ln 2 \left(\frac{\sigma \sigma_1 + h^2 - \sqrt{\sigma_1^2 - h^2}\sqrt{\sigma^2 - h^2}}{\sqrt{\sigma^2 - h^2} - \sqrt{\sigma_1^2 - h^2}} \right) \right.$$

$$- \bar{\sigma}_1 \ln 2 \left(\frac{\sigma \bar{\sigma}_1 + h^2 - \sqrt{\bar{\sigma}_1^2 - h^2}\sqrt{\sigma^2 - h^2}}{\sqrt{\sigma^2 - h^2} + \sqrt{\bar{\sigma}_1^2 - h^2}} \right) - \sqrt{\sigma_1^2 - h^2} \ln \frac{2}{h} (\sigma + \sqrt{\sigma^2 - h^2})$$

$$\left. \left. - \sqrt{\bar{\sigma}_1^2 - h^2} \ln \frac{2}{h} (\sigma + \sqrt{\sigma^2 - h^2}) \right] \right\} + H_5 W_{11} \qquad (43)$$

Where

$$H_5 = -\frac{1}{4} \left\{ \left(\frac{\Gamma\lambda}{\pi} \right)'' 2 (\ln 2 - 1) + H_1 + \left(\frac{h^2}{2} \right)'' + \left[\left(\frac{2\Gamma\lambda}{\pi} + h^2 \right) \ln \frac{2}{h} \right]'' \right\}$$

$$- \frac{1}{4\pi} \left\{ \bar{P}'(s) \left(\frac{1}{4} + \frac{1}{2} \ln \frac{2}{\beta} \right) + \frac{1}{2} \left(\bar{P}'(-1) \ln (1+s) \right. \right. \qquad (44)$$

$$\left. \left. + \bar{P}''(-1) \left[(1+s) \ln (1+s) - (1+s) \right] + \int_{-1}^{s} \bar{P}'''(s_0) \left[(s - s_0) \ln (s - s_0) - (s - s_0) \right] d s_0 \right) \right\}$$

and

$$H_1 = -R.P. \frac{\partial^2}{\partial s^2} \left[\frac{\Gamma}{\pi} \sigma_1 \ln 2 (\sigma_1 + \sqrt{\sigma_1^2 - h^2}) - \frac{\Gamma}{\pi} \bar{\sigma}_1 \ln 2 (\bar{\sigma}_1 - \sqrt{\bar{\sigma}_1^2 - h^2}) \right] \qquad (45)$$

The log term, $\Phi^{\dot{\mu}}_{122}$, is determined by inspection to be

$$\Phi^{\dot{\mu}}_{122} = R.P. \frac{\beta^3 \bar{P}'(s)}{8\pi} W_{11} \tag{46}$$

ψ_1 is then known to fourth order in terms of the small quantities near the body (i.e. through terms of order $a^2 \sin^2\alpha$ and $a^3 \sin\alpha$). This is sufficient for purposes of evaluating the pressure coefficient on the body. That is, it is not necessary to determine ϕ°_{12} to obtain the desired degree of approximation on the body surface.

Solution for ψ_4 and Straining

The partial differential equation for ψ_4 is Equation (10)

$$L(\psi_4) = 2\psi_{1\eta}\psi_{1\eta s} M^2 + 2M^2 \psi_{1\xi}\psi_{1\xi s} + 2\xi_{1\eta}\psi_{1s\eta} + 2\xi_{1\xi}\psi_{1\xi s} + K\psi_{1s}\psi_{1ss} + 2(1-M^2)\xi_{1s}\psi_{1ss} \tag{47}$$

where

$$K = M^2[2 - M^2(1-\gamma)]$$

Both ξ_1 and ψ_4 are to be determined by the matched asymptotic expansion technique. By substitution of the known results for ψ_1 in the right-hand side of Equation (47), it can be seen that far from the body the outer solutions are of the form

$$\psi_4 \sim a^2 \phi^{\circ}_4(\eta, \zeta, s) + \cdots \tag{48a}$$

and

$$\xi_1^{\circ} \sim \xi_1^{\circ}(\eta, \zeta, s) + \cdots \tag{48b}$$

It is also known that the $\psi_{1_S}\ \psi_{1_{SS}}$ term in Equation (47) leads to particular solutions proportional to η (see Reference 7). The terms are then unbounded far from the wing and are obviously not of second order in the far field. The straining should then eliminate the $\psi_{1_S}\ \psi_{1_{SS}}$ term from Equation (47). To accomplish this let

$$\xi_1^\circ = \bar{K}\ \psi_1^\circ \tag{49}$$

where $\bar{K} = \dfrac{K}{2\beta^2}$

then Equation (47) reduces to

$$L\ (\phi_4^\circ) = 2\ (M^2 + \bar{K})\ \phi^\circ_{11_{\eta S}} \tag{50}$$

which has the particular solution

$$\phi_4^\circ = (M^2 + \bar{K})\ \eta\ \phi^\circ_{11_S} \tag{51}$$

Near the body the inner solutions are of form

$$\psi_4 \sim a^2\ \dot{\Phi}^{\dot{\nu}}_{41}(Y, Z, S) + \ldots . \tag{52}$$

$$\xi_1 \sim a\ \dot{\xi}_1^{\dot{\nu}} + \ldots . \tag{53}$$

and Equation (47) reduces to

$$\dot{\Phi}^{\dot{\nu}}_{41_{YY}} + \dot{\Phi}^{\dot{\nu}}_{41_{ZZ}} = 2\left[\dot{\xi}^{\dot{\nu}}_{1_Y}\ \dot{\Phi}^{\dot{\nu}}_{11_{YS}} + \dot{\xi}^{\dot{\nu}}_{1_Z}\ \dot{\Phi}^{\dot{\nu}}_{11_{ZS}}\right] + 2M^2\left[\dot{\Phi}^{\dot{\nu}}_{11_Y}\ \dot{\Phi}^{\dot{\nu}}_{11_{YS}} + \dot{\Phi}^{\dot{\nu}}_{11_Z}\ \dot{\Phi}^{\dot{\nu}}_{11_{ZS}}\right] \tag{54}$$

This can be solved in a similar fashion to Equation (27) by letting $\dot{\Phi}^{\dot{\nu}}_{41} = R.P.\ W_{41}(\sigma, \bar{\sigma})$ then the particular portion of W_{41} is

$$W_{41}(P) = \frac{M^2}{4}\ \frac{\partial}{\partial S}\left[W_{11}(\sigma)\ \overline{W_{11}(\sigma)}\right] + \frac{1}{4}\ \overline{\dot{\xi}_1^{\dot{\nu}}}\ \frac{\partial W_{11}}{\partial S} + \frac{1}{4}\ \dot{\xi}_1^{\dot{\nu}}\ \frac{\partial \overline{W_{11}}}{\partial S} \tag{55}$$

When the complementary portion is added to satisfy the boundary condition or the body surface (Equation (15)), the result is

$$W_{41} = \frac{M^2}{4}\frac{\partial}{\partial S}\left[W_{11}(\sigma)\left(\overline{W_{11}(\sigma)} + W_{11}(\sigma)\right)\right] + \tag{56}$$

$$+ \frac{1}{4}\left(\overline{\xi_1^{\cdot\cdot}} + \xi_1^{\cdot\cdot}\right)\frac{\partial W_{11}}{\partial S} + \frac{\xi_1^{\cdot\cdot}}{4}\left(\frac{\overline{\partial W_{11}}}{\partial S} + \frac{\partial W_{11}}{\partial S}\right)$$

Thus far the solution for ψ_4 is general in that Equation (56) can be obtained without specifically knowing W_{11} .

The first term on the right-hand side of Equation (56) leads to nonintegrable singularities in surface pressure at the leading edge. This can be remedied by letting

$$\xi_1^{\cdot\cdot} = -M^2 W_{11} + F_1 \tag{57}$$

where F_1 is a function which allows matching and whose value and S derivative vanish on the wing surface. Matching the outer expansion of Equation (56) with the inner expansion of Equation (51), F_1 is determine as

$$F_1 = -i\left(M^2 + \bar{K}\right)\left[\sigma - \frac{1}{\sigma}\left(\frac{h^2}{2} + \frac{\Gamma\lambda}{\pi}\right)\right] \tag{58}$$

ψ_4 is now determined through sufficient order in small quantities.

The first term of Equation (57) is seen to be essentially the straining proposed by Sugo in Reference 11 for the subsonic leading edge case. The second term of Equation (57) vanishes on the wing but is needed to correct the nonuniformities in the far field. It is thus seen that Sugo's approximations should be valid near the wing.

The results for no leading edge separation may be extracted from the previous analysis by formally letting $\Gamma = 0$.

It will be noted that the first term in the inner expansion of ψ_4 is proportional to a^2 . The term ψ_4 is then fourth order in terms of small

quantities as were both $\dot{\Phi}^{\dot{\nu}}_{121}$ and $\dot{\Phi}^{\dot{\nu}}_{122}$. The first correction for the nonlinear terms neglected in the linear theory are then the same order as the first nonslenderness correction to slender wing theory.

Pressure Coefficient

The inner solutions for ψ_1 and ψ_4 have been used to calculate wing surface pressures. The corresponding form of Equation (18) is

$$C_p = -2 \sin\alpha \cos\alpha \left(a \dot{\Phi}^{\dot{\nu}}_{11_S} + a^3 \dot{\Phi}^{\dot{\nu}}_{121_S} + a^3 \ln a \, \dot{\Phi}^{\dot{\nu}}_{122_S} \right)$$

$$- \sin^2\alpha \left\{ \dot{\Phi}^{\dot{\nu}\,2}_{11_Z} - 1 + 2\dot{\Phi}^{\dot{\nu}}_{11_Z} \left(a^2 \dot{\Phi}^{\dot{\nu}}_{121_Z} + a^2 \ln a \, \dot{\Phi}^{\dot{\nu}}_{122_Z} \right) \right.$$

$$\left. + a^2 \left[(1-M^2) \dot{\Phi}^{\dot{\nu}\,2}_{11_S} - 2\cos\alpha \left(\dot{\Phi}^{\dot{\nu}}_{11_S} \dot{\xi}^{\dot{\nu}}_{1_S} - \dot{\Phi}^{\dot{\nu}}_{41_S} \right) \right] \right\} \qquad (59)$$

The details of evaluating this expression are given in Appendix C. The normal force coefficient C_N has been evaluated by numerical integration of this expression over the wing surface.

VI. RESULTS AND COMPARISON WITH EXPERIMENT

A comparison of the theory with experimental normal force coefficients from Reference 15 is shown in Figures 4 through 6. The theory is compared with the experimental lift coefficients on an aspect ratio one-quarter wing in Figure 7. These unpublished data were supplied by Charles H. Fox, Jr., NASA Langley Research Center.

It can be seen that although the second order theory represents a significant improvement over the slender wing results of Reference 2, the normal force is still overpredicted. In general the agreement between experiment and the second order theory is best at the lower angles of attack and higher Mach numbers. This is readily seen when the normal force results are plotted versus Mach number as has been done in Figures 8 and 9. Also shown in these figures are the theoretical results for the case without leading edge separation. The exact linear theory result with no leading edge separation is given by:

$$C_N = \sin\alpha \cos\alpha \frac{\pi A}{E(k)} ; \quad \beta A \leq 4 \tag{60}$$

where $E(k)$ is the complete elliptic integral of the second kind with modulus k given by

$$k = \sqrt{1 - \left(\frac{\beta A}{4}\right)^2} \tag{61}$$

The corresponding second order theory result may be obtained with the use of Equation 59 as

$$C_N = \sin\alpha \cos\alpha \frac{\pi A}{2} \left\{1 + \frac{\beta^2 A^2}{32}\left(\frac{1}{2} + \ln\frac{\beta A}{16}\right)\right\} \tag{62}$$

(This corresponds to the results obtained in Reference 16.) Equations 60 and 62 are shown in Figures 8 and 9.

When the leading edge becomes sonic, Equation 60 approaches the linearized theory values for a supersonic leading edge which are given by:

$$C_N = \sin\alpha \cos\alpha \frac{4}{\beta} ; \quad \beta A \geq 4 \tag{63}$$

The findings of Reference 17 indicate that Equation 63 is in fairly good agreement with the data for supersonic leading edge wings and slightly over predicts normal force for sonic edge wings. The second order theory with leading edge separation is then seen to approach the theory without leading edge separation (and the data level) as the leading edge becomes supersonic. The second order theory then approaches approximately the correct level at a sonic leading edge which is consistent with the vanishing of the vortex lift as the leading edge becomes supersonic.

It should be noted that neither the exact linear theory nor the second order theory is strictly applicable in the immediate neighborhood of a sonic leading edge. Neither theory incorporates the proper interaction between the shock wave and wing that is important when the shock is near the leading edge. The straining employed in the second order theory partially accounts for this interaction; however, for proper consideration the shock would require explicit treatment in the cross flow problem.

The Mach number trend predicted by the second order theory is evidently correct because both the slenderness and nonlinear correction terms of the second order solution attempt to regain the hyperbolic character of the governing partial differential equations that had been lost in the slender wing approximation. The outer solution satisfies the wave equation and therefore exhibits the hyperbolic character of supersonic flow. (That is the property that the disturbances propagated from a point are confined to its downstream Mach cone.) The matching between inner and outer solutions then partially transmits this character to the inner solution.

The normal force behavior exhibited in Figures 4 through 9 may be understood further by examining the surface pressure distributions and wing loading distributions. Comparisons between theoretical and experimental spanwise pressure distributions from Reference 18 are shown in Figures 10 and 11. The theoretical predictions from Reference 4 are included in these figures because of the more exact representation of the spiral vortex sheet used in that analysis. This inclusion required some compromise since only limited results were presented in Reference 4 and experimental pressure distributions

at precisely these conditions were not available. The upper surface pressure distribution from Reference 4 shown in Figure 10 was obtained by interpolation from the presented results. The theoretical results shown in Figure 11 are for values of $A = 1.0$ and $\bar{\epsilon} = 1.0$ while the experimental data are for $A = 1.07$ and $\bar{\epsilon} = 1.02$. These discrepancies were not felt to be significant and do not obscure the overall trends.

It is apparent from these comparisons that all the theories grossly overestimate the magnitude of the upper surface suction peak. The more exact representation of the spiral vortex sheet used in Reference 4 provides only a modest improvement in the functional form of the spanwise pressure distribution. The magnitude of the suction peak is overpredicted because the predicted vortex locations are too close to the wing surface. The peak is most pronounced at the lower angles as is seen in Figure 12.

As seen in Figure 11, under certain conditions the predicted upper surface pressure peak exceeds the vacuum level which is a physical impossibility. This is an indication that the expansion procedure which was used to obtain the approximate form of the pressure coefficient, Equation 59, from the exact relation, Equation 17, has broken down. This, however, is evidently not the fundamental failing of the theory since the suction peak is overpredicted even in those cases where the vacuum limit has not been exceeded (as in Figure 10). The discrepancy in functional form between the theory and experiment indicates that the cross flow model used, even in the case of Reference 4, is inadequate. The flatness of the experimental pressure distribution in the leading edge vicinity would suggest that secondary separation is important and should probably be modeled as a long leading edge bubble.

For values of βA below approximately 3 the second order theory pressure and loading distributions have essentially the same character as the slender wing theory, Reference 2. This may be seen in Figure 12. (The quantity ΔC_p used in Figures 12 through 14 is the difference between upper and lower surface pressure coefficients.) At higher values of βA, however, the peak is greatly reduced. As seen in Figures 13 and 14 the predominant corrections to slender wing theory occur in the vicinity of the suction peak.

The loading along the wing center line where the best correlation in surface pressures is obtained is only slightly affected by the second order corrections. The second order theory then primarily operates on the vortex lift and acts to improve the agreement between theory and experiment. However, the initial slender wing estimate has the wrong functional form and cannot be sufficiently corrected to agree with the experimental pressure distributions. Improvements are therefore required in the cross flow model to improve correlation.

A comparison of the nonslenderness and nonlinear correction term contributions to normal force and pressure distribution can be made. If the ψ_4 term and straining are dropped from the expansion procedure the remaining higher order terms of the solution correct only for the slenderness assumptions. That is, the remaining solution is an approximation to the exact linearized flow problem. The predicted normal forces from these two versions of the theory are shown in Figure 15 for an aspect ratio 1.0 wing. In general, the difference between the two theories is small except at small angles of attack and higher Mach numbers where the full second order theory predicts higher normal force. The discrepancy at low angles of attack was unexpected. The reasons for these differences, however, may be seen in Figure 16 where the theoretically predicted upper surface pressures for one case in this angle range are shown. The corrections to account for the nonlinear terms in the equations of motion accentuate the peak of the upper surface pressure distribution. Since this peak is most prevalent in the theory at low angles of attack, the largest discrepancies in normal force occur there. The discrepancy at higher angles of attack is generally less significant.

No moments have been calculated because the solutions for delta wings are conical and hence the aerodynamic center is located at two-thirds the root chord. The application of the leading edge Kutta condition prohibits the development of any axial force, and therefore normal force is the only remaining pressure force on the wing.

VII. CONCLUSIONS

A second order theory has been developed for calculating the supersonic flow about slender wings with leading edge separation. The theory has been developed as a correction to slender wing theory. The Brown and Michael cross flow model has been used to model the leading edge separation effects. Second order theory provides substantial improvement over the conventional slender wing results for normal force but is still higher than experiment. In general at moderate Mach numbers the slender wing error in normal force is halved by the second order corrections.

The theory shows the reduction of vortex lift with Mach number, approaching the proper levels as the leading edge becomes sonic, and also demonstrates an improved aspect ratio variation.

Agreement between theoretical and experimental pressure distributions is inhibited by the limitations of the cross flow model used. A suitable representation of the region of secondary separation near the leading edge is required before significant improvements in the theoretically predicted pressure distributions can be expected.

APPENDIX A

MATCHED ASYMPTOTIC EXPANSION AND STRAINED COORDINATE TECHNIQUES

A brief outline is given of the two perturbation techniques. The present report is the first known combined application of these techniques. This was necessitated in view of the difficulties that are encountered in the straightforward application of the matched asymptotic expansion technique to supersonic flow problems. Van Dyke discusses these difficulties in Section 7, Chapter 6 of Reference 6. He developed a method to overcome these problems for the two-dimensional case. His technique could, however, not be extended to general three-dimensional problems and necessitated the development of the present theory.

The terminology of perturbation theory as defined in Reference 6 is used throughout this report.

The theory of matched asymptotic expansions was originally developed for viscous flow problems. The fundamental details and original development of the technique may be found in Reference 19. An additional reference where applications to some nonviscous flow problems are considered is Reference 6. Briefly, the fundamental ideas involved may be described as follows. It is assumed that the velocity potential can be expanded in a series in some small parameter, ϵ, (in the present application, this parameter is the ratio of wing span to wing chord) and, furthermore, that this solution can be divided into two parts: one part, valid for small ϵ far from the wing, called the outer solution and the other part, valid for small ϵ near the wing, called the inner solution. In general, the inner and outer solutions cannot be completely determined from the boundary conditions which apply to each solution. This incompleteness is resolved by requiring certain compatability between the solutions referred to as the matching conditions. Following the notation of Reference 6, the outer solution is denoted by $\phi^{\bullet}$ and the inner solution by $\bar{\phi}^{\dot{\imath}}$. It is assumed that the outer solution may be expanded in

an asymptotic series as

$$\phi^{\circ} = \phi^{\circ}(x, y, z; \epsilon) \sim \psi_{o}^{\circ} + f_{1}(\epsilon)\,\phi_{1}^{\circ} + f_{2}(\epsilon)\,\phi_{2}^{\circ} + \cdots f_{n}(\epsilon)\,\phi_{n}^{\circ} + \cdots \quad \text{(A-1)}$$

where

$$\phi_{i}^{\circ} = \phi_{i}^{\circ}(x, y, z) \quad ; \qquad i = 1, 2, \cdots n \cdots$$

The first m terms of this expansion will be called the m term outer expansion. Here, x, y, z are referred to as outer variables and are chosen such that the leading term is not a function of ϵ . (They are generally the unaltered physical variables of the problem.) The f_{i} are referred to as gage functions and have the property that

$$\lim_{\epsilon \to 0} \frac{f_{n+1}}{f_{n}} = 0 \qquad \text{(A-2)}$$

Similarly, it is assumed that the inner solution may be expanded in an asymptotic series as

$$\bar{\Phi}^{i} = \bar{\Phi}^{i}(X, Y, Z; \epsilon) = \bar{\Phi}_{o}^{i} + f_{1}(\epsilon)\,\bar{\Phi}_{1}^{i} + f_{2}(\epsilon)\,\bar{\Phi}_{2}^{i} + \cdots f_{n}(\epsilon)\,\bar{\Phi}_{n}^{i} + \cdots \quad \text{(A-3)}$$

The first m terms of this expansion are referred to as the m term inner expansion. The inner variables, X, Y, Z are chosen such that the leading term is not a function of ϵ and again

$$\lim_{\epsilon \to 0} \frac{f_{n+1}}{f_{n}} = 0 \qquad \text{(A-4)}$$

The inner and outer variables are related by a function of ϵ . The expansion obtained by substituting inner variables in the m term outer expansion, expanding for small ϵ and retaining the first n terms is called the n term inner expansion of the m term outer solution. This is abbreviated as

" n inner (m outer)". Similarly, the n term outer expansion of the m term inner solution is formed by substituting outer variables in the m term inner solution and expanding to n terms. This is abbreviated as " n outer (m inner)". The matching required between inner and outer solutions can then be stated as:

$$m \text{ outer } (n \text{ inner}) = n \text{ inner } (m \text{ outer})$$

This is the asymptotic matching principle as presented in Reference 6.

The method of strained coordinates was orginally devised by Lighthill and Whitham for problems involving the location of bow shock waves in supersonic flow. The development is given in Reference 8. The basic idea is that the first order solution may have the proper form, but not at the proper values of the independent variables (coordinates). This is remedied by expanding one or more of the independent variables as well as the solution in an asymptotic series. Thus, in addition to expanding the solution in the form of Equation (A-1), one of the independent variables, say x is expanded as

$$x \sim s + f_1(\epsilon)\, \xi_1 + \cdots f_n(\epsilon)\, \xi_n + \cdots \qquad \text{(A-5)}$$

where

$$\xi_i = \xi_i(s, y, z) \qquad \text{(A-6)}$$

The functions ξ_i are called the strainings and are determined step by step as part of the solution. The strainings are determined by the principle that:

Higher approximations shall be no more singular than the first.

APPENDIX B

SLENDER WING SOLUTION FOR BICONVEX CIRCULAR ARC PROFILE WING

The slender wing solution has been obtained for a conical wing with biconvex circular arc profile in the cross flow plane. Certain fundamental difficulties were encountered in obtaining the second order solution and have not as yet been overcome. However, since no theoretical results are available for thick wings with leading edge separation, the slender wing results are presented along with a discussion of the problems associated with the extension of the solution to higher order.

The general formulation and expansion procedures for thick wings is given in Section IV of this report.

The conventional slender wing result is the first term in the inner expansion of ψ_1 . The inner variables are selected as in the infinitely thin case and the problem reduces to the quasi two-dimensional problem in the cross flow plane in precisely the same fashion. The partial differential equation for $\overset{\cdot}{\Phi}^{\cdot}_{11}$ is

$$\overset{\cdot}{\Phi}^{\cdot}_{11_{YY}} + \overset{\cdot}{\Phi}^{\cdot}_{11_{ZZ}} = 0 \qquad \text{(B-1)}$$

with boundary conditions

$$\mathcal{S}_Y \overset{\cdot}{\Phi}^{\cdot}_{11_Y} + \mathcal{S}_Z \overset{\cdot}{\Phi}^{\cdot}_{11_Z} = 0 \qquad \text{on} \qquad \mathcal{S} = 0 \qquad \text{(B-2)}$$

For the biconvex profile $\epsilon = a$ and the surface ordinates are given by

$$\frac{1}{a}\mathcal{S} = \pm Y - h\left[\left(\frac{1+\bar{t}^2}{2\bar{t}}\right)^2 - \left(\frac{Z}{h}\right)^2\right]^{1/2} + h\left(\frac{1-\bar{t}^2}{2\bar{t}}\right) = 0 \qquad \text{(B-3)}$$

where $\bar{t}$ is the ratio of wing half thickness to half span (thickness ratio in cross flow plane). (The plus sign in Equation B-3 applies to the upper surface and the minus sign to the lower.) The quantity $\bar{t}$ is assumed to be of order

one and for a conical wing is a constant. This thickness ratio may be expressed in terms of θ, the edge angle, by $\bar{t} = \frac{1 - \cos \theta/2}{\sin \theta/2}$

The Brown and Michael representation of the spiral vortex sheet is used. The cross flow model is shown in Figure 17A. The spiral vortex sheets are represented by a concentrated vortex of strength Γ and $-\Gamma$ located at σ_1 and $-\bar{\sigma}_1$ respectively. A cut extends from the leading edge to each corresponding vortex. The cross flow problem is easily handled by conformal transformations.

Let $\Phi_{11}^{i} = R.P.\ w_{11}(\sigma)$ (B-4)

The transformation

$$\frac{\zeta}{d} = \frac{1 + \left(\frac{\sigma - h}{\sigma + h}\right)^{1/k}}{1 - \left(\frac{\sigma - h}{\sigma + h}\right)^{1/k}} \tag{B-5}$$

transforms the biconvex profile to a circle of diameter d in the ζ plane. (See Reference 20) such that

$$k d = h . \tag{B-6}$$

The case for $k = 2$ corresponds to a flat plate and the following analysis reduces to the analysis of Reference 2 in this case. In the ζ plane the solution is known (See Reference 21) as

$$w_{11}(\zeta) = -i \left\{ \zeta - \frac{d^2}{\zeta} + \frac{\Gamma}{2\pi} \left[\ln(\zeta - \zeta_1) + \ln\left(\zeta + \frac{d^2}{\zeta_1}\right) - \ln(\zeta + \bar{\zeta}_1) - \ln\left(\zeta - \frac{d^2}{\bar{\zeta}_1}\right) \right] \right\} \tag{B-7}$$

The ζ plane is shown in Figure 17B. The transformed vortex location ζ_1 and Γ remain to be determined by the overall force balance on each vortex and cut and the Kutta condition at the leading edge. The surface boundary conditions are automatically satisfied by the properties of the

conformal transformation. The cut in the cross flow potential represents a vortex sheet where the vorticity is aligned perpendicular to the freestream. The Kutta-Joukowsky force produced on this sheet by the freestream must balance the Kutta-Joukowsky force produced on the concentrated vortex by the velocities in the cross flow plane. This may be expressed as

$$\frac{d\Gamma}{ds}\left(\bar{\sigma}_1 - h\right) = \Gamma\left(\left.\frac{d\,\mathcal{W}_{11}}{d\sigma}\right|_{\sigma=\sigma_1} - \frac{d\sigma_1}{ds}\right) \tag{B-8}$$

where $\left.\frac{d\,\mathcal{W}_{11}}{d\sigma}\right|_{\sigma=\sigma_1}$ is the complex cross flow velocity evaluated at σ_1 without the contribution of the vortex located at σ_1 .

The smooth outflow from the leading edge or leading edge Kutta condition is given by

$$\left.\frac{d\,\mathcal{W}_{11}}{d\sigma}\right|_{\sigma=h} = 0 \tag{B-9}$$

Using Equation (B-6) for $\mathcal{W}_{11}$ these conditions can be specifically formulated. The force balance is

$$\bar{\epsilon}\left(2\,\frac{\bar{\sigma}_1}{h} - 1\right) = -i\left\{\left(1 + \frac{d^2}{\zeta_1^2}\right) + \frac{\Gamma}{2\pi}\left[\frac{\zeta_1}{\zeta_1^2 + d^2} - \frac{1}{\zeta_1 + \bar{\zeta}_1} - \frac{\bar{\zeta}_1}{\zeta_1\bar{\zeta}_1 - d^2}\right]\right\}\left(\frac{\zeta_1^2 - d^2}{\sigma_1^2 - h^2}\right) + i\,\frac{\Gamma}{2\pi}\left(\frac{\zeta_1 - \sigma_1}{\sigma_1^2 - h^2}\right) \tag{B-10}$$

where $\bar{\epsilon} = \frac{\sin\alpha}{\tan\Lambda}$ and Λ is the wing semi apex angle. The Kutta condition is

$$\frac{\Gamma}{2\pi}\left[\frac{\zeta_1}{\zeta_1^2 - d^2} + \frac{\bar{\zeta}_1}{\bar{\zeta}_1^2 - d^2}\right] = 1 \tag{B-11}$$

ζ_1 is available from Equation (B-5) as

$$\zeta_1 = \alpha \left[\frac{1 + \left(\frac{\sigma_1 - h}{\sigma_1 + h} \right)^{1/k}}{1 - \left(\frac{\sigma_1 - h}{\sigma_1 + h} \right)^{1/k}} \right] \tag{B-12}$$

For specified values of the parameters $\bar{\epsilon}$ and k these three equations constitute a system of three nonlinear complex algebraic equations for the three unknowns σ_1, ζ_1, and $\frac{\Gamma}{h}$. This system has been solved numerically. The resulting values of vortex positions are shown in Figure 18. The resulting values for vortex strength are shown in Figure 19. It is noticed that for a given value of $\bar{\epsilon}$ the vortex is pushed further outboard and drawn closer to the wing surface with thickness. No pressure distributions have been calculated but, since the vortex is closer to the wing and further outboard for a given value of $\bar{\epsilon}$, no improvement in the upper surface pressure peak can be expected. The slender wing normal force results have, however, been calculated. Using the momentum theorem the normal force may be expressed as

$$C_N = \pi A \bar{G}_2 \sin\alpha \cos\alpha \tag{B-13}$$

where

$$\bar{G}_2 = \frac{1}{k^2} \left(\frac{2 + k^2}{3} \right) + \frac{\Gamma}{2\pi} \left(\zeta_1 + \bar{\zeta}_1 \right) \left\{ 1 - \frac{1}{k^2 \zeta_1 \bar{\zeta}_1} \right\} \tag{B-14}$$

The normal force parameter $\bar{G}_2$ has been plotted in Figure 20. The first term in $\bar{G}_2$, Equation (B-14), corresponds to the unseparated result and the second term accounts for the vortex lift. The unseparated lift increases with thickness and the vortex lift decreases with thickness producing the crossovers at low $\bar{\epsilon}$ in Figure 20.

As seen in Section IV of this report the first order lifting and non-lifting problems separate. The slender wing thickness solution is then the first term in the inner expansion for ψ_2. This problem is also easily solved by

conformal mapping. The solution in the ζ plane is a source, i.e.

$$W_{21} = B \ln \zeta \tag{B-15}$$

where

$$\Phi_{21}^{\dot{\nu}} = R.P. W_{21} \tag{B-16}$$

The constant B is determined from the boundary condition , Equation (13), as

$$B = \hbar k (1 + \bar{t}) \frac{\bar{t}}{2} \cos \alpha \sin \frac{\theta_4}{k} \tag{B-17a}$$

where

$$\theta_4 = \tan^{-1} \frac{2\bar{t}}{1 - \bar{t}} \quad ; \quad 0 \leq \theta_4 \leq \frac{\pi}{2} \tag{B-17b}$$

Again no thickness pressures have been calculated. However, it is easily seen that the thickness pressure will be singular at the leading edge whereas the application of the Kutta condition has removed the leading edge singularity from the lifting portion of the solution.

It should also be noted that in the present expansion scheme the ψ_2 solution does not affect the ψ_1 solution. That is, there is no cross flow velocity contribution from the source term (Equation (B-15)) in the force balance (Equation (B-10)) as is present in the analysis of Bryson (Reference 21).

It may then be concluded that the inclusion of thickness in the flow model will result in lower normal force but will not improve the form of the pressure distributions.

The problems of extending the solution for the biconvex profile to higher order are associated with the determination of the particular portion of $\dot{\Phi}_{121}^{\nu}$. These problems are demonstrated in the following. The partial differential equation for $\dot{\Phi}_{121}^{\nu}$ is Equation (27). Following the previous

fashion for solving this equation the general solution for the particular portion of W_{121} can be expressed in the form of an indefinite integral as

$$W_{121}(P) = \left(\frac{M^2-1}{4}\right) \frac{\partial^2}{\partial S^2} \left\{ \bar{\sigma} \int \overline{w_{11}(\sigma)}\, d\sigma + \sigma \int \overline{w_{11}(\sigma)}\, d\bar{\sigma} \right\} \quad \text{(B-18)}$$

The integrals appearing in Equation (B-18) can only be evaluated analytically for a few select values of k . The outer limit of Equation (B-18) is needed for matching with the outer solution. The limiting process and integration operation cannot in general be interchanged as is shown by the following example for the case of unseparated flow about a flat wing ($k = 2.0$).

$$\text{Let} \quad W_{11} = -i\sqrt{\sigma^2 - k^2} \quad \text{(B-19a)}$$

in outer variables this is

$$W_{11} = -i\sqrt{\frac{\xi^2}{a^2} - k^2} \quad ; \quad (\xi = a\sigma) \quad \text{(B-19b)}$$

then

$$\lim_{a\to 0} \int W_{11}\, d\sigma = \lim_{a\to 0} -i \left\{ \frac{1}{2} \frac{\xi}{a} \sqrt{\left(\frac{\xi}{a}\right)^2 - k^2} \right. \quad \text{(B-20)}$$

$$\left. - \frac{k^2}{2} \ln \left[\frac{\xi}{a} + \sqrt{\left(\frac{\xi}{a}\right)^2 - k^2} \right] \right\} = -i \left[\frac{\xi^2}{2a^2} - \frac{k^2}{4} - \frac{k^2}{2} \ln\left(2\frac{\xi}{a}\right) \right]$$

and

$$\int \lim_{a\to 0} W_{11}\, d\sigma = -\frac{i}{a} \int \frac{\xi}{a} \left(1 - \frac{1}{2} \frac{a k^2}{\xi^2}\right) d\xi \quad \text{(B-21)}$$

$$= -\frac{i}{a} \left(\frac{\xi^2}{2a} - \frac{1}{2} a k^2 \ln \xi \right)$$

Comparison of Equations (B-21) and (B-20) indicates that the constant terms (those terms not involving ξ) are not faithfully reproduced when the limit process and integration order are reversed. An additional constraint is needed to uniquely determine the constants of integration in the expansion procedure. At present this constraint is unknown. The work on this aspect of the problem was, however, not pursued further since the full second order solution for the flat wing had been obtained and it did not appear that the inclusion of thickness in the cross flow problem would substantially improve the correlation of wing surface pressures.

APPENDIX C

PRESSURE DISTRIBUTION FOR INFINITELY THIN WING

The pressure distribution is found from the evaluation of Equation (59). It is first noted that on the wing surface the following terms do not contribute to the pressure coefficient:

1) The $\bar{\Phi}^{\dot{}}_{41_S}$ term
2) The particular portion (Equation (41)) of $\bar{\Phi}^{\dot{}}_{121}$
3) The F_1 term of $\bar{\xi}^{\dot{}}_1$ (Equation (58))

With these simplifications and the assumption of conical flow, Equation (59) reduces to

$$C_p = -2 \sin\alpha \cos\alpha \left\{ a + a^3 H_5 + a^3 \ln a\, H_6 \right\} \bar{\Phi}^{\dot{}}_{11_S} \qquad \text{(C-1)}$$

$$- \sin^2\alpha \left\{ (1 + 2a^2 H_5 + 2a^2 H_6)\, \bar{\Phi}^{\dot{}\,2}_{11_2} + (2\cos\alpha M^2 - \beta^2)\, a^2 \bar{\Phi}^{\dot{}\,2}_{11_S} - 1 \right\}$$

where for conical flow

$$H_5 = \frac{1}{4}\left(A_1 + \frac{1}{2}\right)\left(1 + \ln\frac{\beta}{8}\right) - \frac{1}{16} - \frac{A_1}{4}\left\{ \ln 2 - 1 - \frac{\tilde{p}}{4\tilde{\lambda}} \ln\frac{R_1}{R_2} + \frac{\tilde{q}}{2\tilde{\lambda}}\left(\beta_1 + \beta_2\right) \right\} \qquad \text{(C-2)}$$

$$A_1 = \tilde{\lambda}^2 + \tilde{\tau}^2 \qquad \text{(C-3)}$$

$$R_1 = (\tilde{p} + \tilde{\lambda})^2 + (\tilde{q} + \tilde{\lambda})^2 \qquad \text{(C-4)}$$

$$R_2 = (\tilde{p} - \tilde{\lambda})^2 + (\tilde{\tau} - \tilde{q})^2 \qquad \text{(C-5)}$$

$$\beta_1 = \tan^{-1}\frac{\tilde{q} + \tilde{\tau}}{\tilde{p} + \tilde{q}} \quad ; \quad 0 \le \beta_1 < \frac{\pi}{2} \qquad \text{(C-6)}$$

$$\beta_2 = \tan^{-1} \frac{\tilde{\tau} - \tilde{q}}{\tilde{p} - \tilde{\lambda}} \quad ; \quad \frac{\pi}{2} \leq \beta_2 < \frac{3\pi}{2} \tag{C-7}$$

$$H_6 = \frac{1}{4} \left(A_1 + \frac{1}{2} \right) \tag{C-8}$$

and the substitution $\sigma_1 = h(\tilde{p} + i\tilde{q})$ has been used. The required derivatives of $\Phi_{11}^{\cdot}$ are

$$\Phi_{11_S}^{\tilde{\cdot}} = R.P. \frac{\partial}{\partial s} W_{11} = \frac{h'}{\pm\sqrt{1+u^2}} \left[1 - \frac{A_1 u^2}{\tilde{\lambda}^2 + (\pm\sqrt{1-u^2} - \tilde{\tau})^2} \right] \tag{C-9}$$

$$+ \frac{A_1}{2\tilde{\lambda}} h' (\theta_1 - \theta_2)$$

$$\Phi_{11_z}^{\tilde{\cdot}} = R.P. \frac{dW_{11}}{d\sigma} = \frac{u}{\pm\sqrt{1-u^2}} \left[\frac{A_1 u^2}{\tilde{\lambda}^2 + (\pm\sqrt{1-u^2} - \tilde{\tau})^2} - 1 \right] \tag{C-10}$$

where

$$u = \frac{z}{h} \tag{C-11}$$

The negative value of $\sqrt{1-u^2}$ is used on the upper wing surface and the positive value is used on the lower wing surface. The angles θ_1 and θ_2 are the arguments of the logarithmic term of W_{11}. The proper branch is most easily selected in the transformed plane $\chi = \sqrt{\sigma^2 - h^2}$. This plane is shown in Figure 21. In this plane the wing transforms to a slit along the imaginary axis from $-ih$ to ih and the concentrated vortices are located at $\sqrt{\sigma_1^2 - h^2}$ and $-\sqrt{\sigma_1^2 - h^2}$. The wing tips transform to the origin and hence the branch cuts in the potential are lines from each vortex to the origin. To confine the discontinuities of the cross flow solution to the cuts and wing surface the function must be defined differently in two domains.

Domain I is defined as $R.P.\ \chi \geq 0$ and Domain II is defined as $R.P.\ \chi \leq 0$.

Domain I then contains the right-hand wing panel and θ_1 and θ_2 are given by

$$\theta_1 = \pi + \alpha_1 \quad ; \quad I.P.\ \chi \geq 0 \quad (upper\ surface) \tag{C-12}$$

and

$$\alpha_1 = \tan^{-1} \frac{\tilde{\tau} - \sqrt{1-u^2}}{\tilde{\lambda}} \quad ; \quad -\frac{\pi}{2} \leq \alpha_1 < \frac{\pi}{2} \tag{C-13}$$

$$\theta_1 = -\pi + \alpha_2 \quad ; \quad I.P.\ \chi \leq 0 \quad (lower\ surface) \tag{C-14}$$

and

$$\alpha_2 = \tan^{-1} \frac{\tilde{\tau} + \sqrt{1+u^2}}{\tilde{\lambda}} \quad ; \quad -\frac{\pi}{2} \leq \alpha_2 < \frac{\pi}{2} \tag{C-15}$$

$$\theta_2 = -\alpha_1 \tag{C-16}$$

A similar scheme is used in Domain II. The resulting composite function is then continuous along the imaginary axis in the χ plane.

From the resulting function then it can be shown that the following expressions are valid across the entire wing span.

On the lower surface

$$\theta_1 - \theta_2 = -\pi - 2\alpha_2 \tag{C-17}$$

and on the upper surface

$$\theta_1 - \theta_2 = \pi + 2\alpha_1 \tag{C-18}$$

The resulting jump in pressure at the wing tips is then consistent with the Kutta-Joukowski force on the feeding sheet.

The normal force on the wing is then found by integrating numerically the pressure jump over the wing area.

It should be noted that in the unseparated flow case where $\dot{\Phi}^{\iota}_{11_S}$ is an odd function of Y that the last term of Equation (C-1) will not contribute to normal force.

REFERENCES

1. Polhamus, E. C., "Predictions of Vortex-Lift Characteristics Based on a Leading Edge Suction Analogy," AIAA Paper No. 69-1133, October 1969.

2. Brown, C. E. and Michael, W. H., Jr., "On Slender Delta Wings with Leading-Edge Separation," NACA TN 3430, April 1955.

3. Mangler, K. W. and Smith, J. H. B., "Calculation of the Flow Past Slender Delta Wings with Leading Edge Separation," R.A.E. Report Aero 2593, May 1957.

4. Smith, J. H. B., "Improved Calculations of Leading-Edge Separation From Slender Delta Wings," R.A.E. Technical Report No. 66070, March 1966.

5. Nenni, J. P. and Tung, C., "A Second-Order Slender-Wing Theory for Wings with Leading Edge Separation," NASA CR-66762, April 1969.

6. Van Dyke, M. D., "Perturbation Methods in Fluid Mechanics," Academic Press, 1964.

7. Van Dyke, M. D., "A Study of Second-Order Supersonic Flow Theory," NACA Report 1081, 1952.

8. Lighthill, M. J., "A Technique for Rendering Approximate Solutions to Physical Problems Uniformly Valid," Z. Flugwiss.9, 1961.

9. Hayes, W. D., "Pseudotransonic Similitude and First-Order Wave Structure," J.A.S. Vol. 21, 1954.

10. Clarkson, M. H., "A Second-Order Theory for Three-Dimensional Wings in Supersonic Flow," Quart. J. Mech. and Appl. Math. 7, 1954.

11. Sugo, M., "The Second-Order Theory of the Three-Dimensional Thin Wing Expansion," T. Moriya Memorial Seminar for Aerodynamics, University of Tokyo, Dept. of Aeronautics, Research Memo 1, 1958.

12. Lee, D. H., "A Second-Order Theory for Supersonic Flow Over Three-Dimensional Wings," M. Sc. Thesis, University of Adelaide, 1963.

13. Pai, S. I., "Introduction to the Theory of Compressible Flow," D. Van Nostrand Co., Inc., 1959.

14. Jones, R. T., "Properties of Low-Aspect-Ratio Pointed Wings at Speeds Below and Above the Speed of Sound," NACA Report 835, 1946.

15. Hill, W. A., Jr., "Experimental Lift of Low-Aspect-Ratio Triangular Wings at Large Angles of Attack and Supersonic Speeds," NACA RM A57117, November 1957.

16. Wang, K. C., "A New Approach to "Not-So-Slender" Wing Theory," Journal of Math. and Physics, Vol. XLVII, No. 4, December 1968.

17. Lampert, S. "Aerodynamic Force Characteristics of Delta Wings at Supersonic Speeds," Jet Propulsion Laboratory Report No. 20-82, September 1954.

18. Michael, W. H., Jr., "Flow Studies on Flat-Plate Delta Wings at Supersonic Speed," NACA TN 3472, July 1955.

19. Lagerstrom, P. A., Howard, L. N., and Liu, C. S., (Editors) "Fluid Mechanics and Singular Perturbations A Collection of Paper by Saul Kaplan," Academic Press, 1967.

20. Milne-Thompson, L. M., "Theoretical Aerodynamics," Macmillan and Company, 1948, pg. 126.

21. Bryson, A. E., "Symmetric Vortex Separation on Circular Cylinders and Cones," Journal of Applied Mechanics, Vol. 26, No. 4, December 1959.

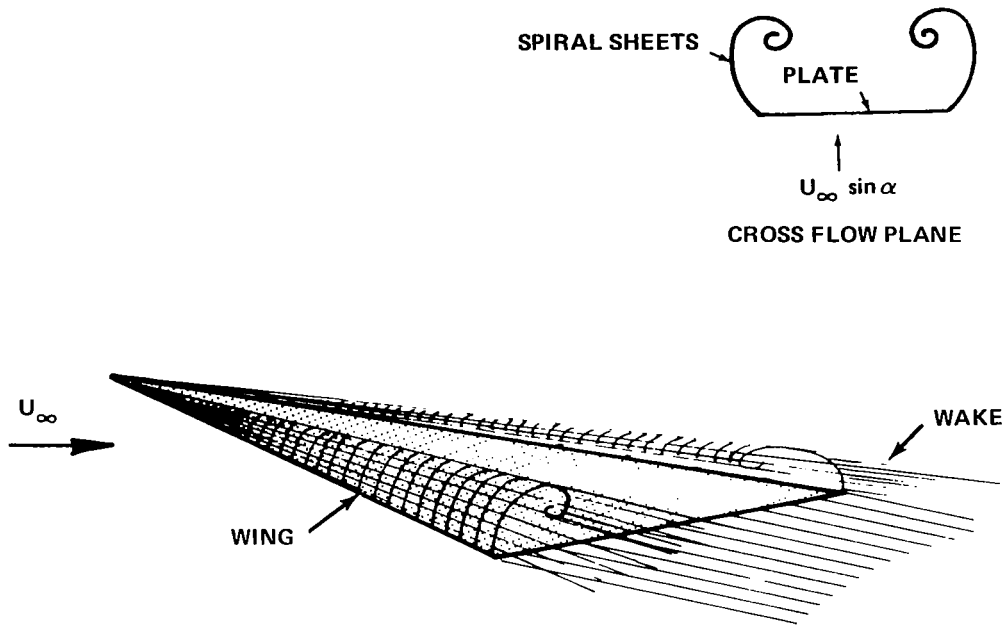

Figure 1 FLOW MODEL WITH LEADING EDGE SEPARATION

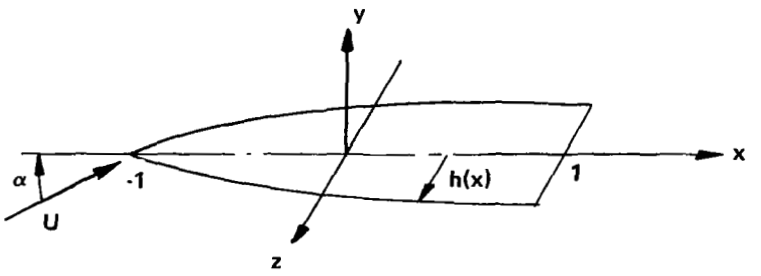

Figure 2 COORDINATE SYSTEM AND WING GEOMETRY

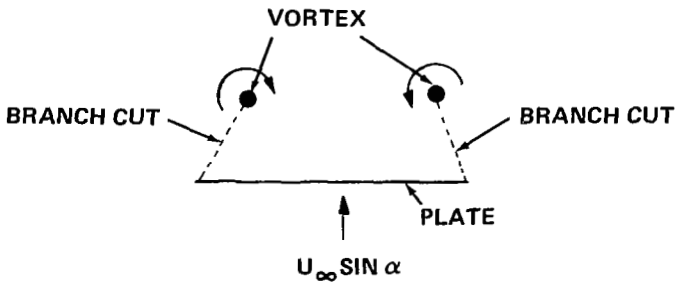

Figure 3 BROWN & MICHAEL FLOW MODEL IN CROSS FLOW PLANE

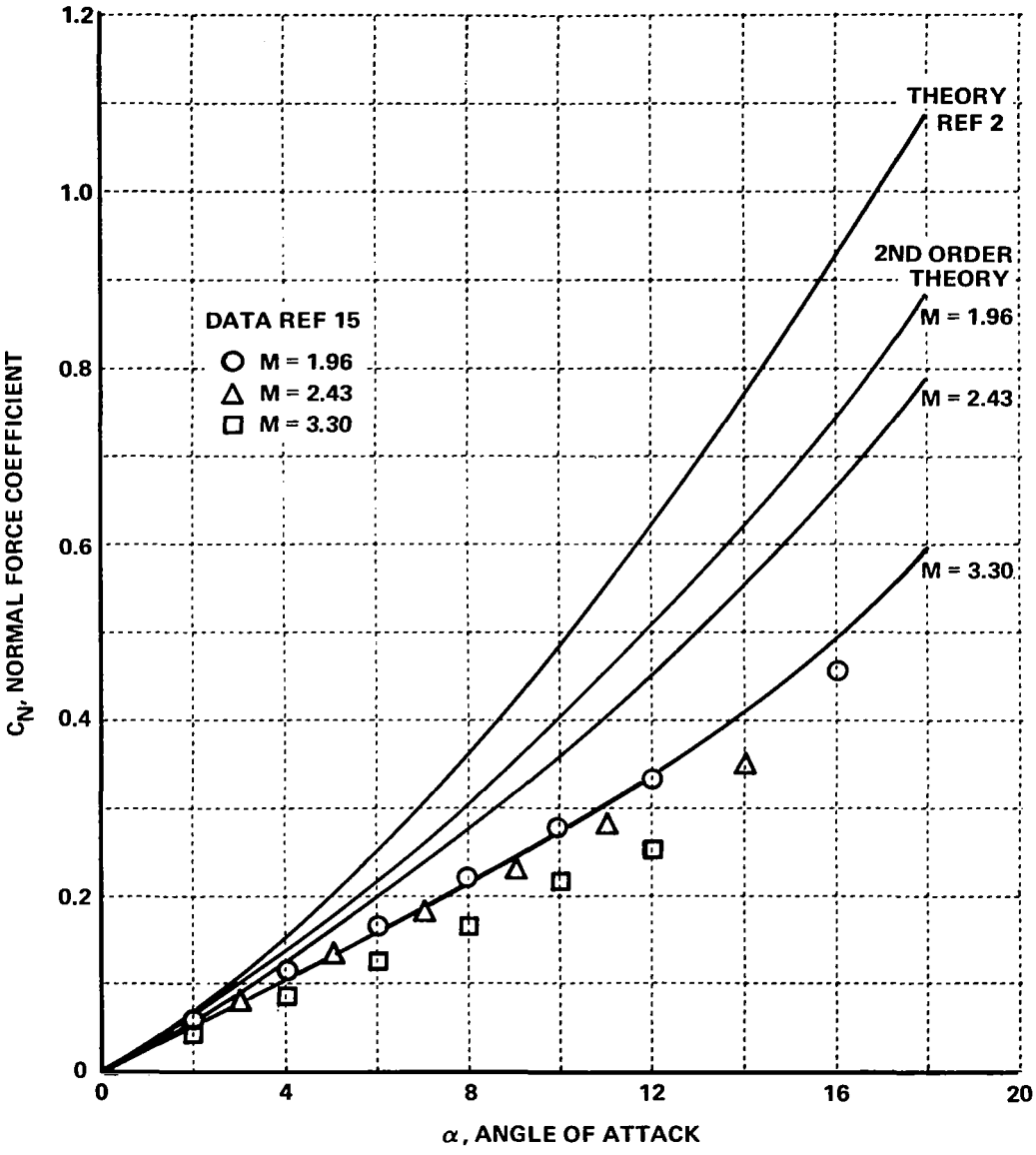

Figure 4 COMPARISON OF THEORY AND EXPERIMENT FOR NORMAL FORCE ON DELTA WINGS, A = 1.0

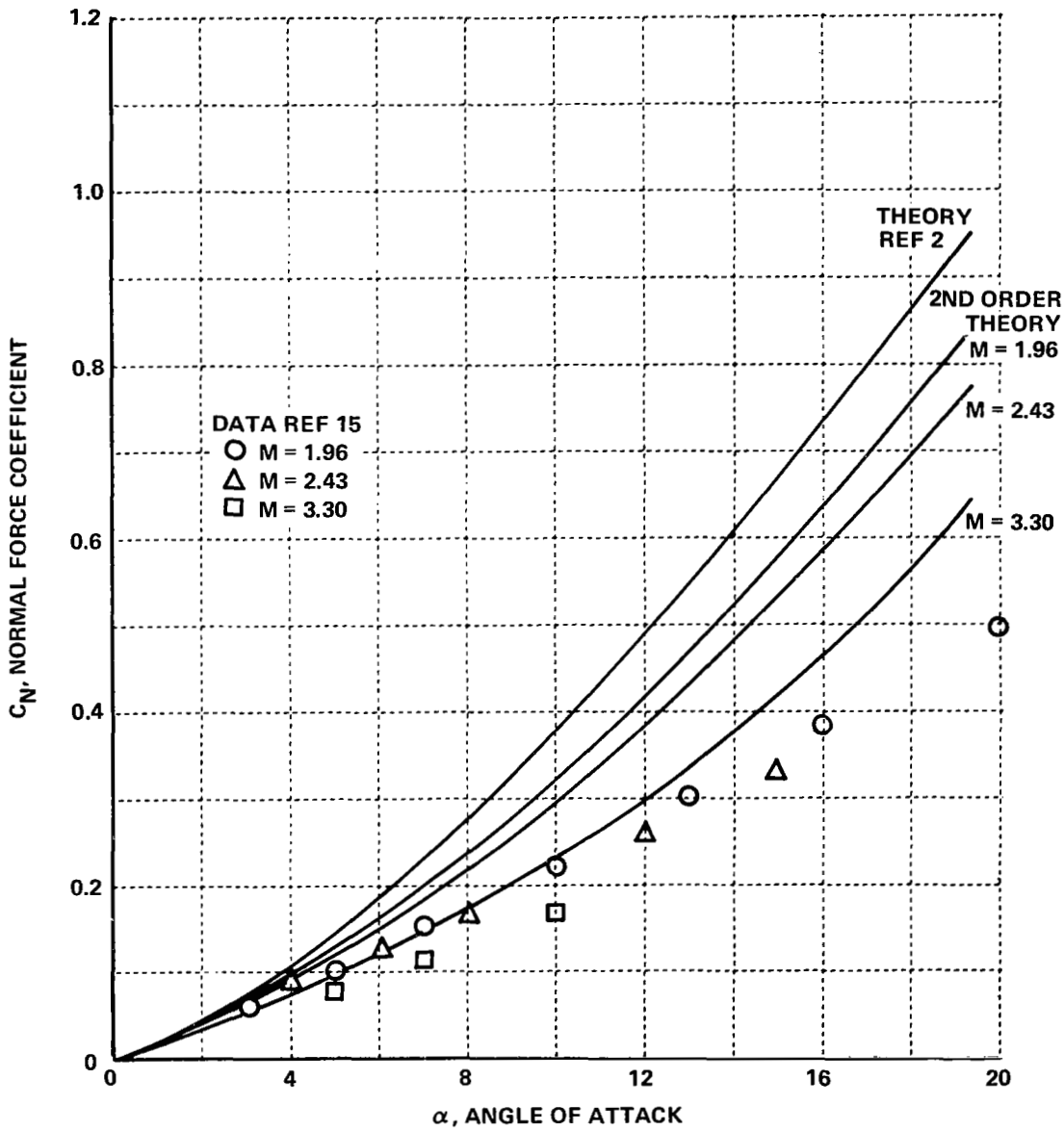

Figure 5 COMPARISON OF THEORY AND EXPERIMENT FOR NORMAL FORCE ON DELTA WINGS, A = 0.667

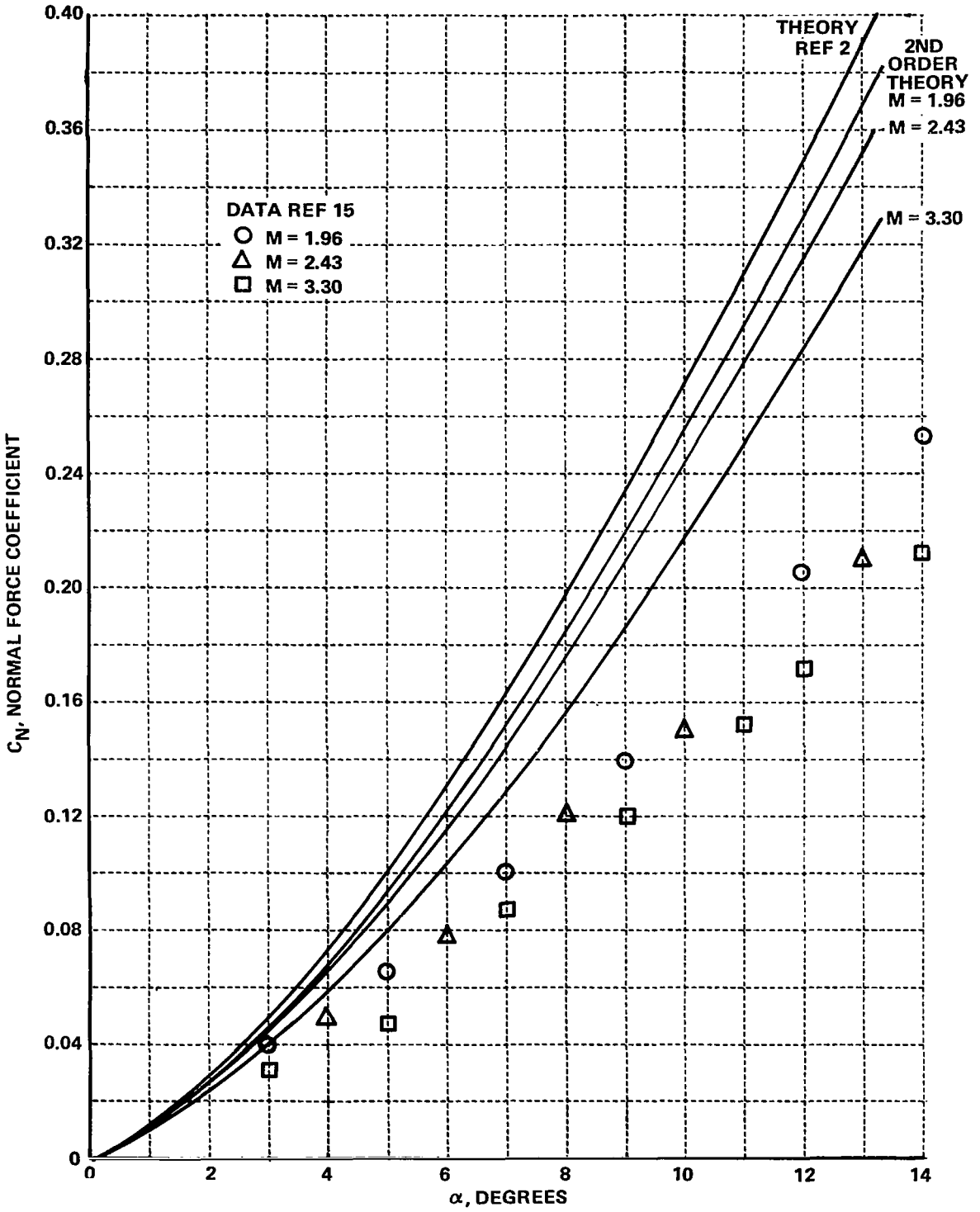

Figure 6 COMPARISON OF THEORY AND EXPERIMENT FOR NORMAL FORCE ON DELTA WINGS, A = 0.375

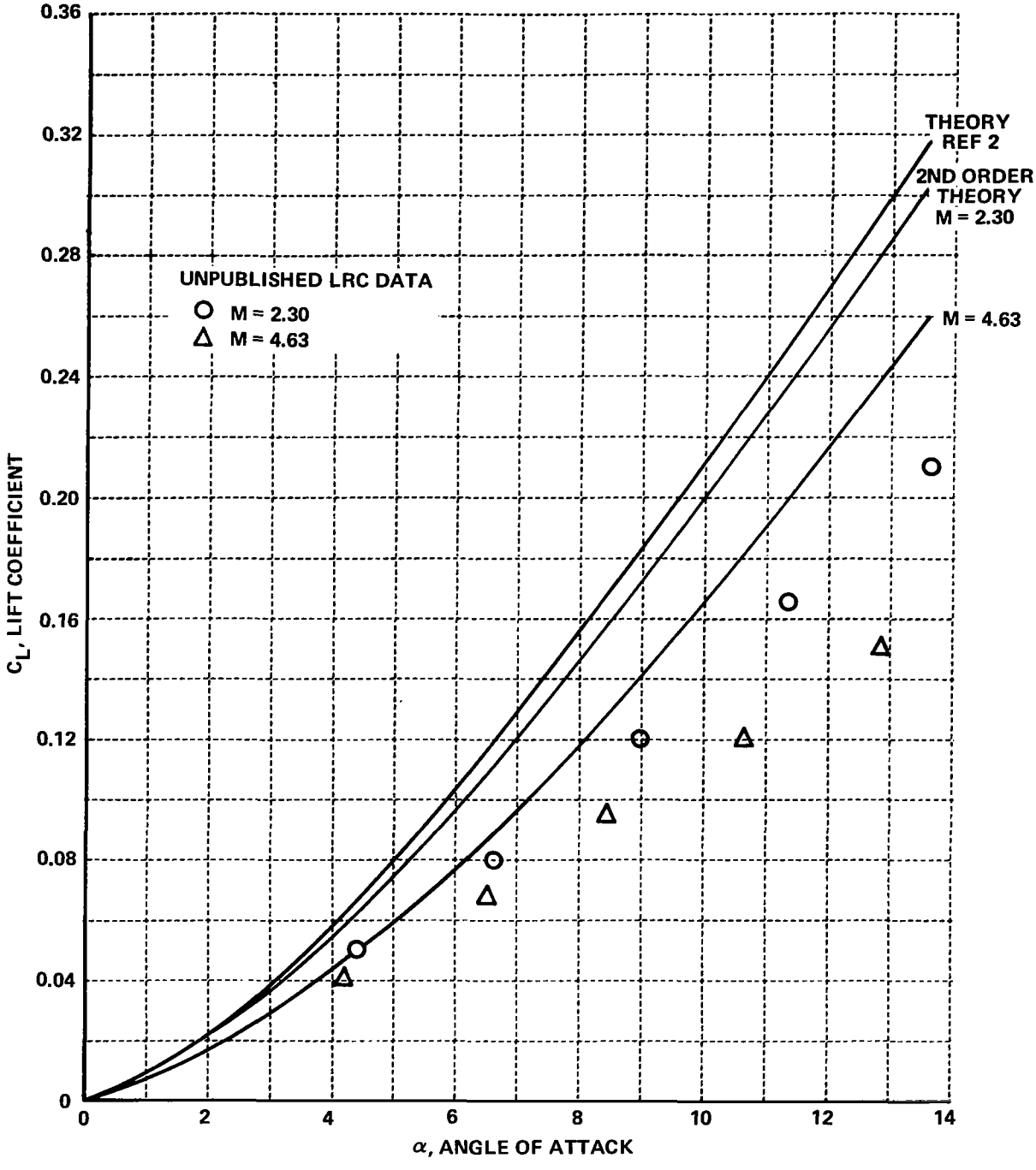

Figure 7 COMPARISON OF THEORY AND EXPERIMENT FOR LIFT ON DELTA WINGS, A = 0.25

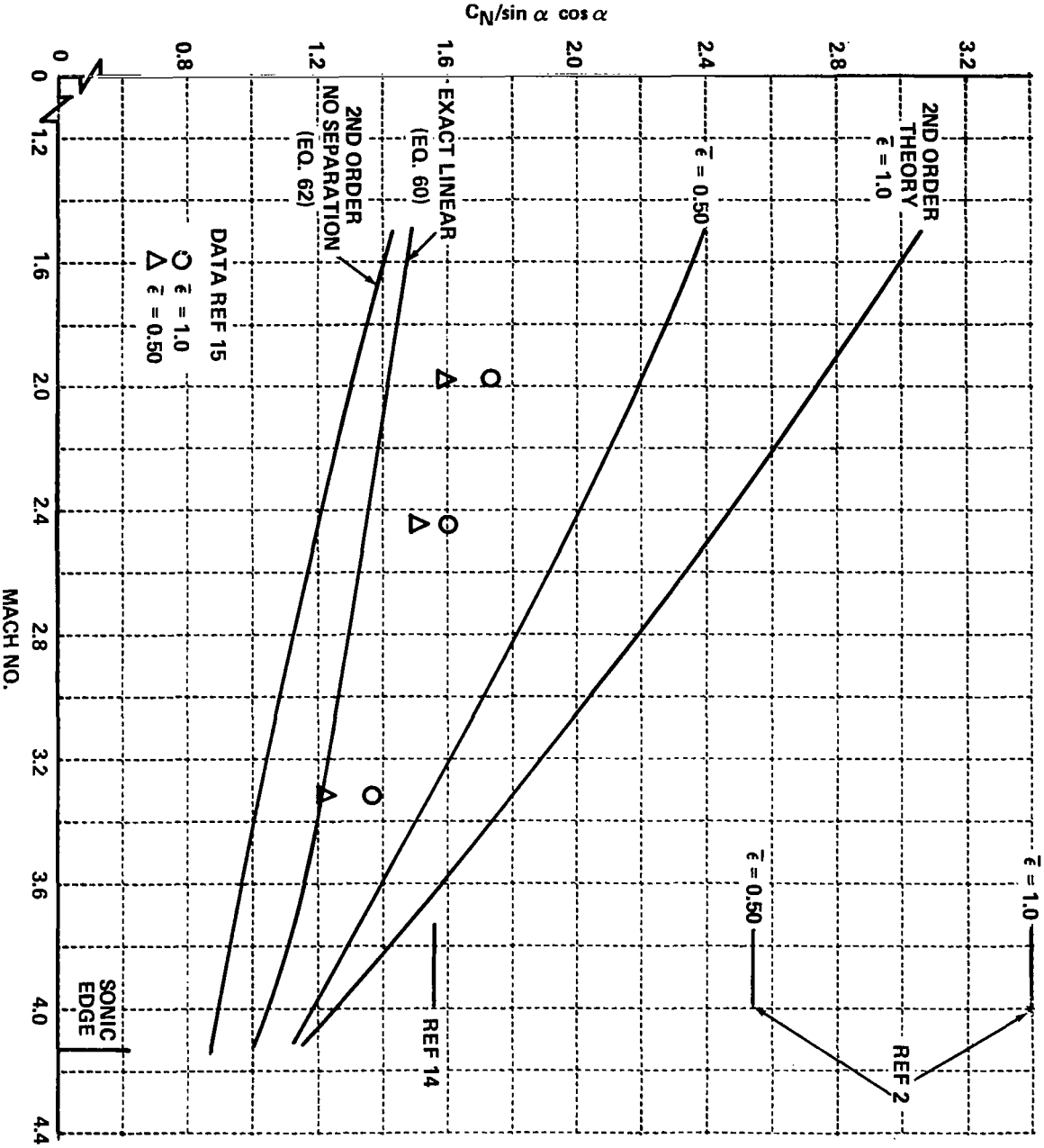

Figure 8 COMPRESSIBILITY EFFECT ON NORMAL FORCE , A = 1.00

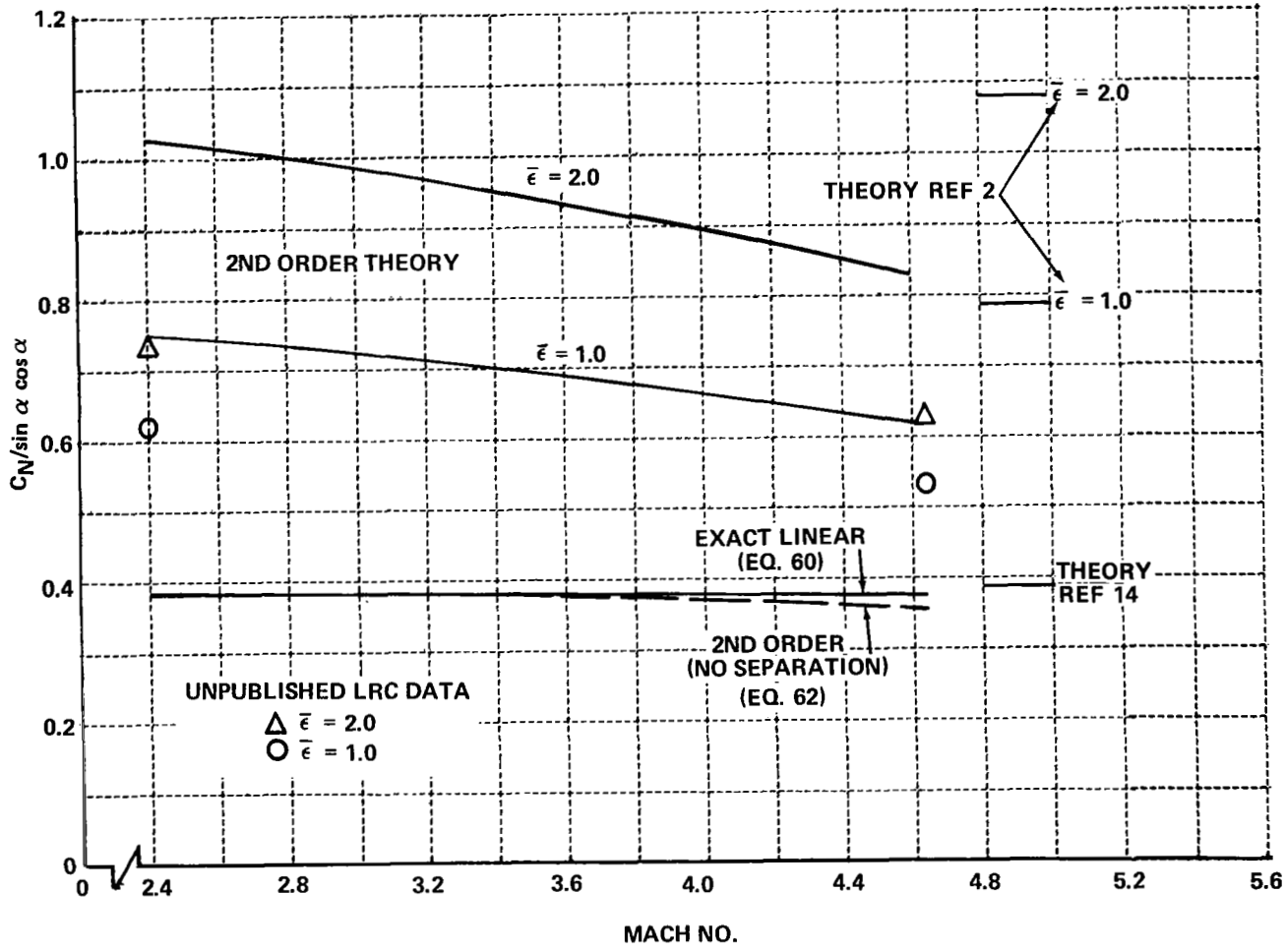

Figure 9 COMPRESSIBILITY EFFECT ON NORMAL FORCE, A = 0.25

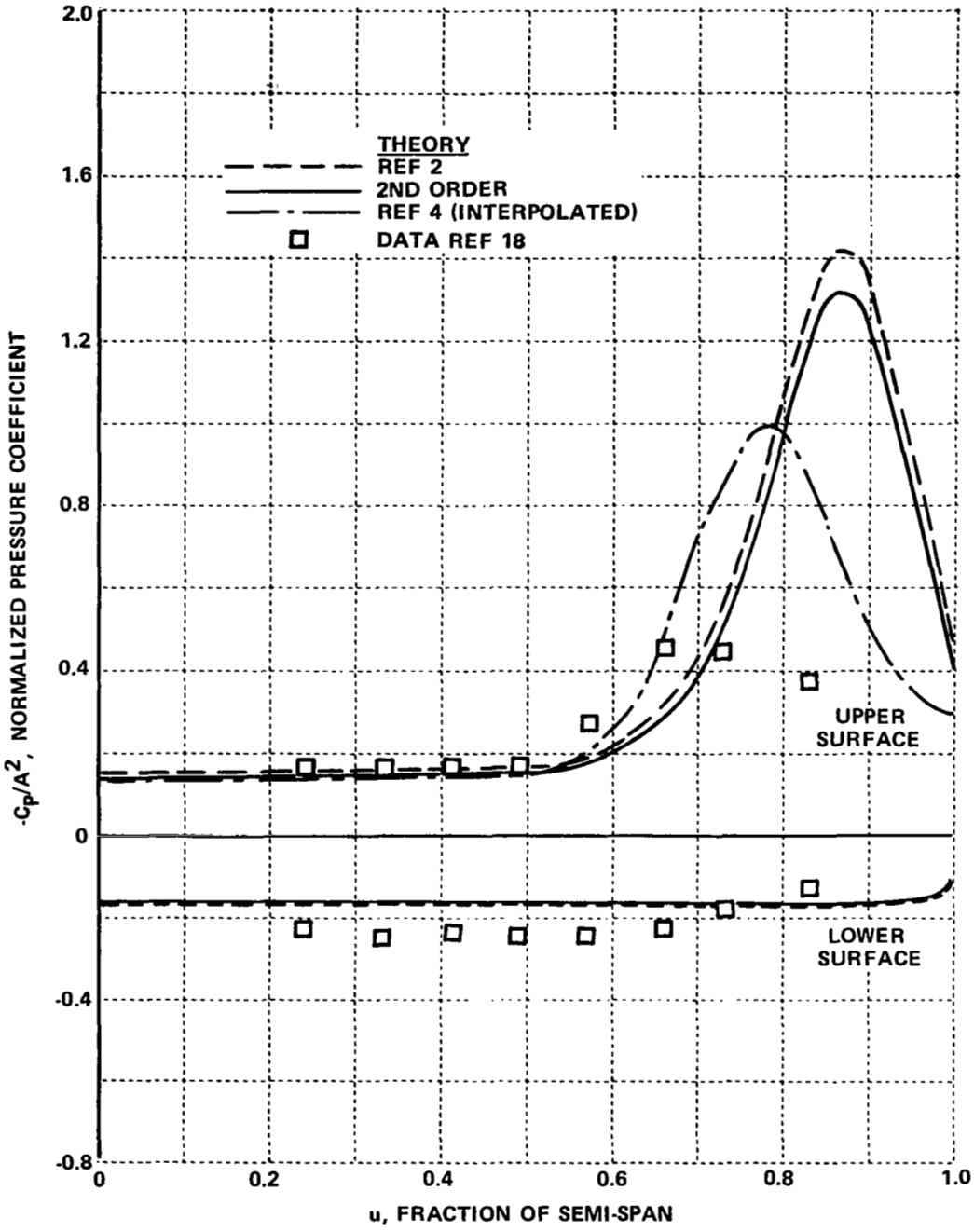

Figure 10 COMPARISON OF THEORETICAL AND EXPERIMENTAL SPANWISE PRESSURE DISTRIBUTIONS, M = 1.9, A = 0.35, $\alpha = 4^{o}$, ($\bar{\epsilon} = 0.8$)

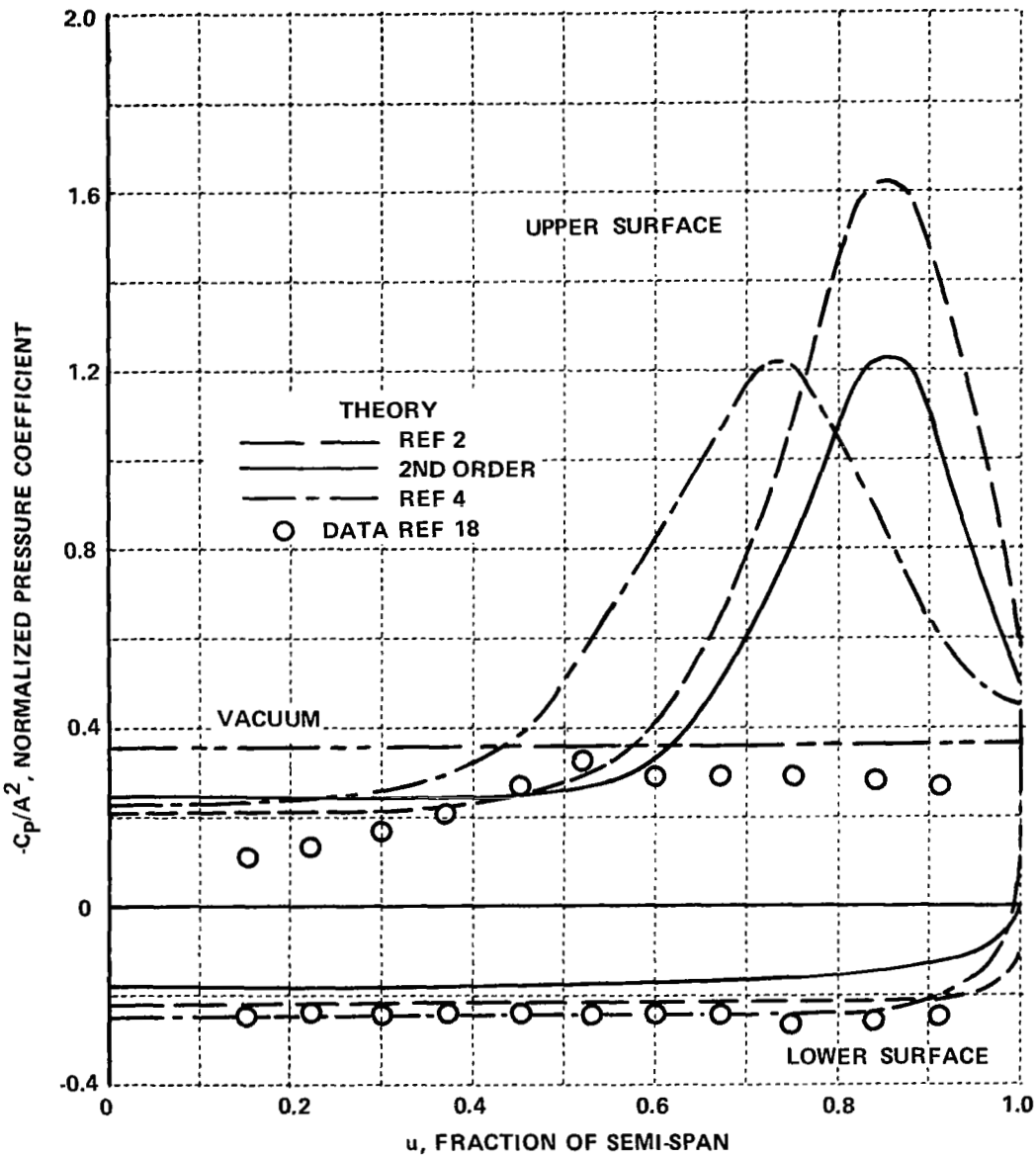

Figure 11 COMPARISON OF THEORETICAL AND EXPERIMENTAL SPANWISE PRESSURE DISTRIBUTIONS, M = 1.9, A ≈ 1.0, $\bar{\epsilon} \approx 1.0$

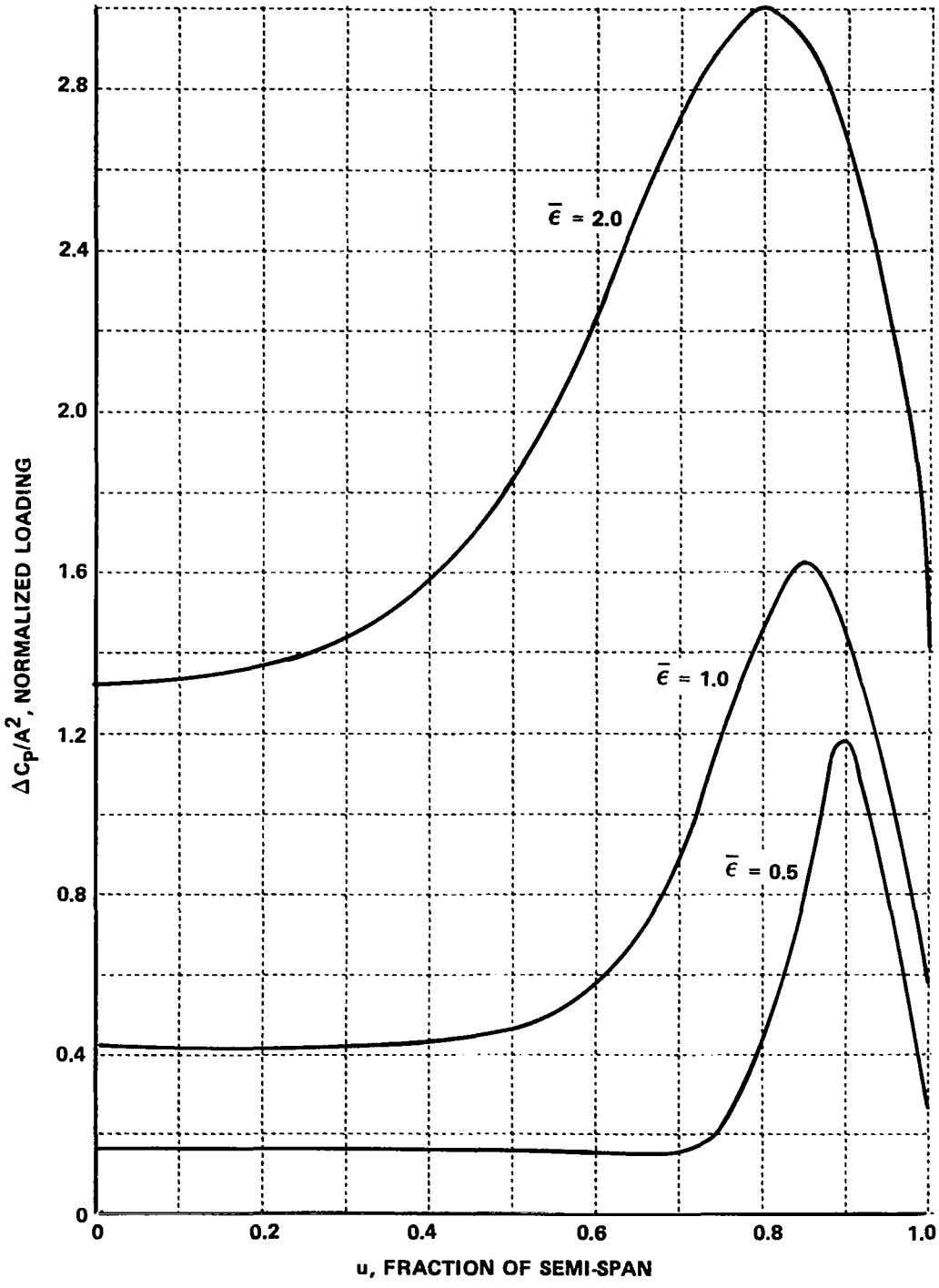

Figure 12 THEORETICAL VARIATION OF WING LOADING WITH ANGLE OF ATTACK A = 1.0, M = 1.5

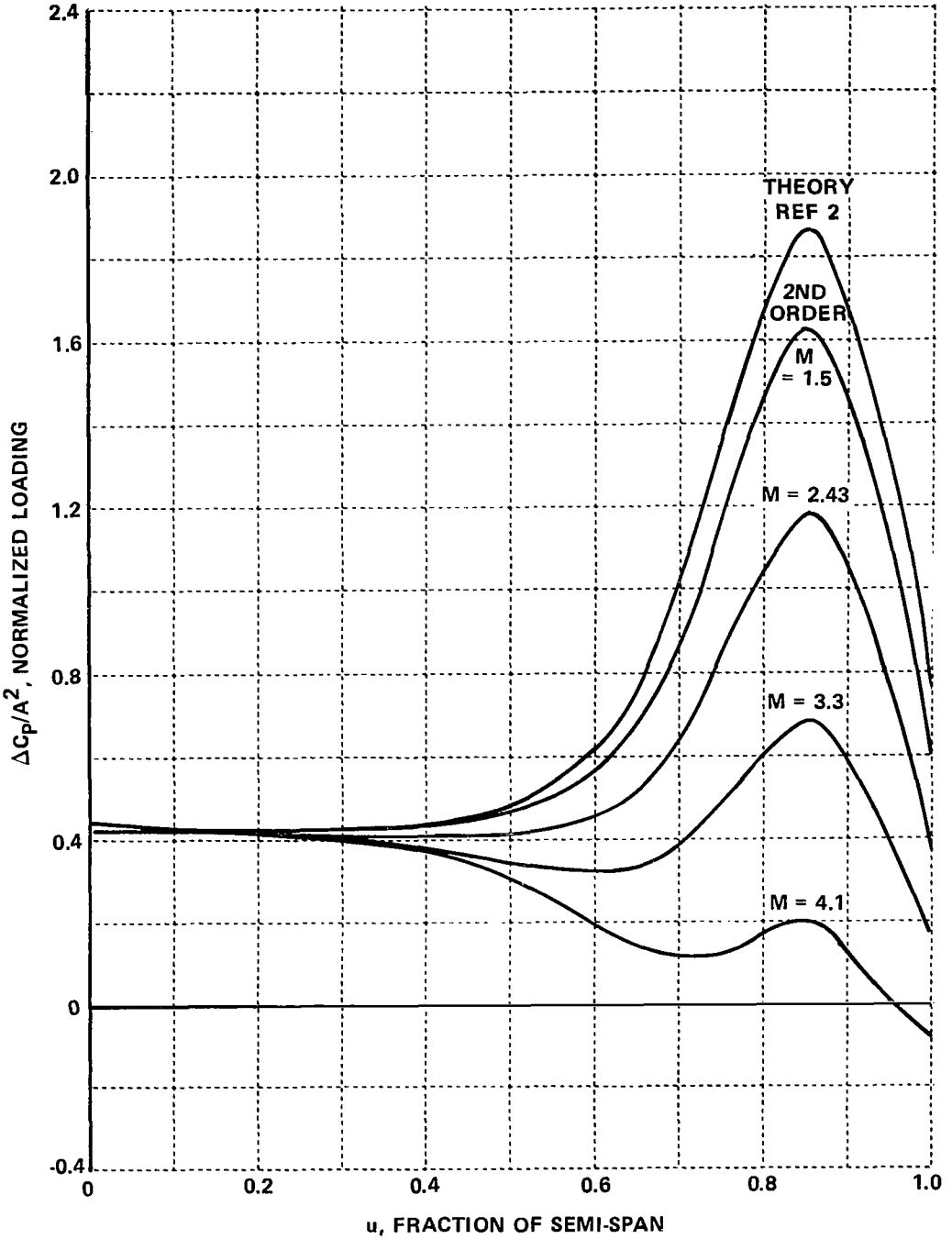

Figure 13 THEORETICAL EFFECT OF MACH NUMBER ON WING LOADING
A = 1.0, $\bar{\epsilon}$ = 1.0

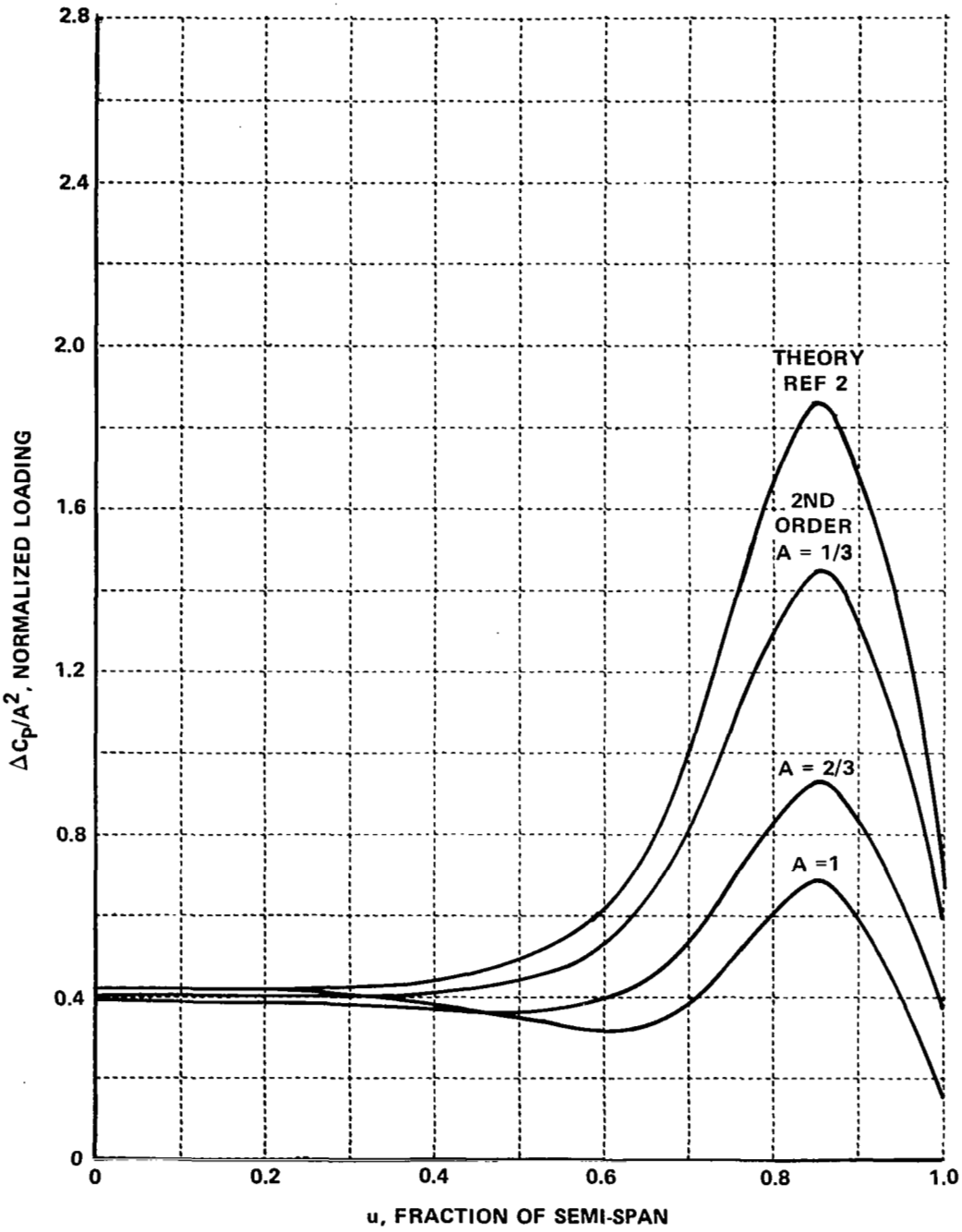

Figure 14 THEORETICAL EFFECT OF ASPECT RATIO ON WING LOADING
M = 3.3, $\bar{\epsilon}$ = 1.0

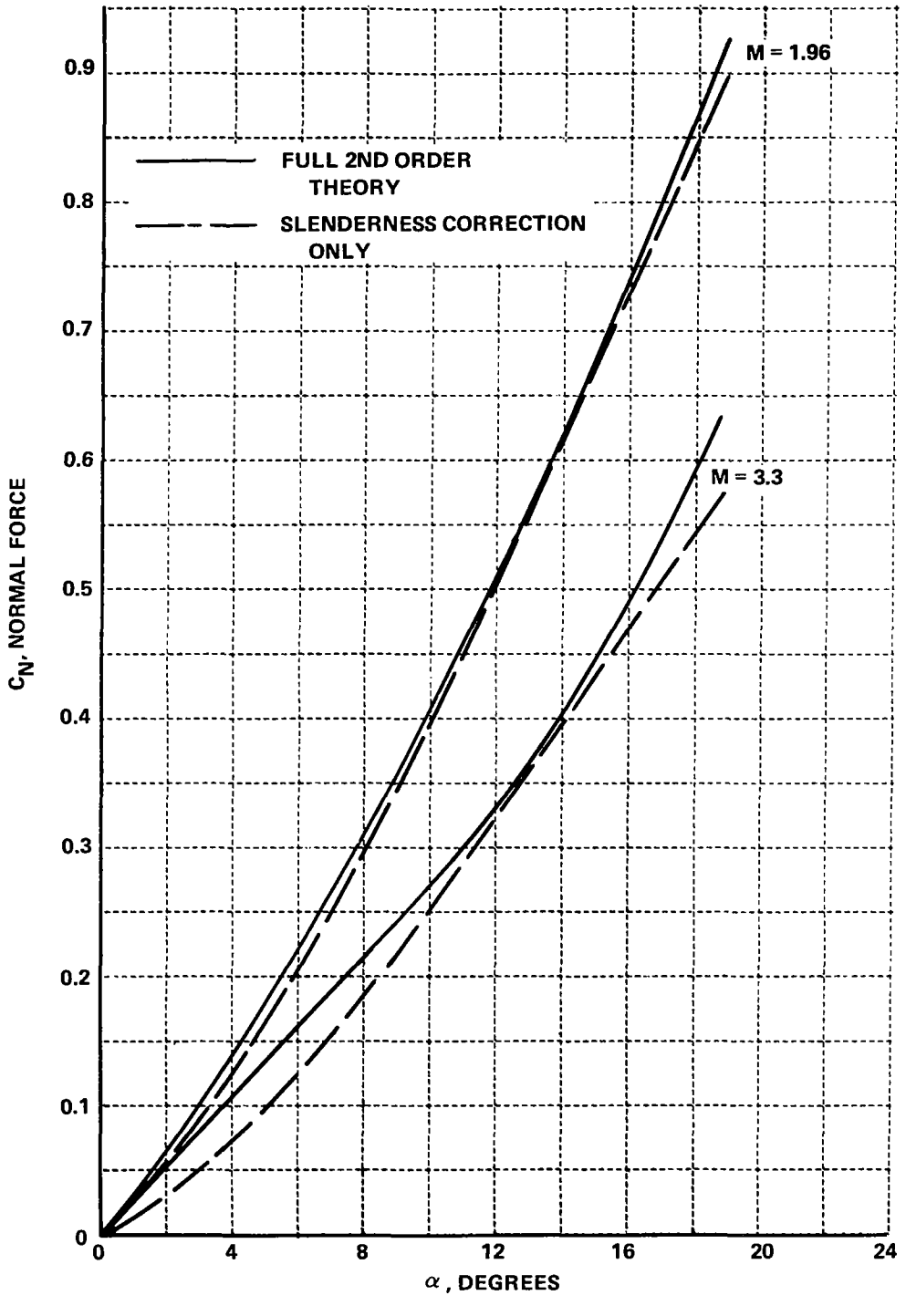

Figure 15 COMPARISON OF THEORETICALLY PREDICTED NORMAL FORCE, A = 1.0

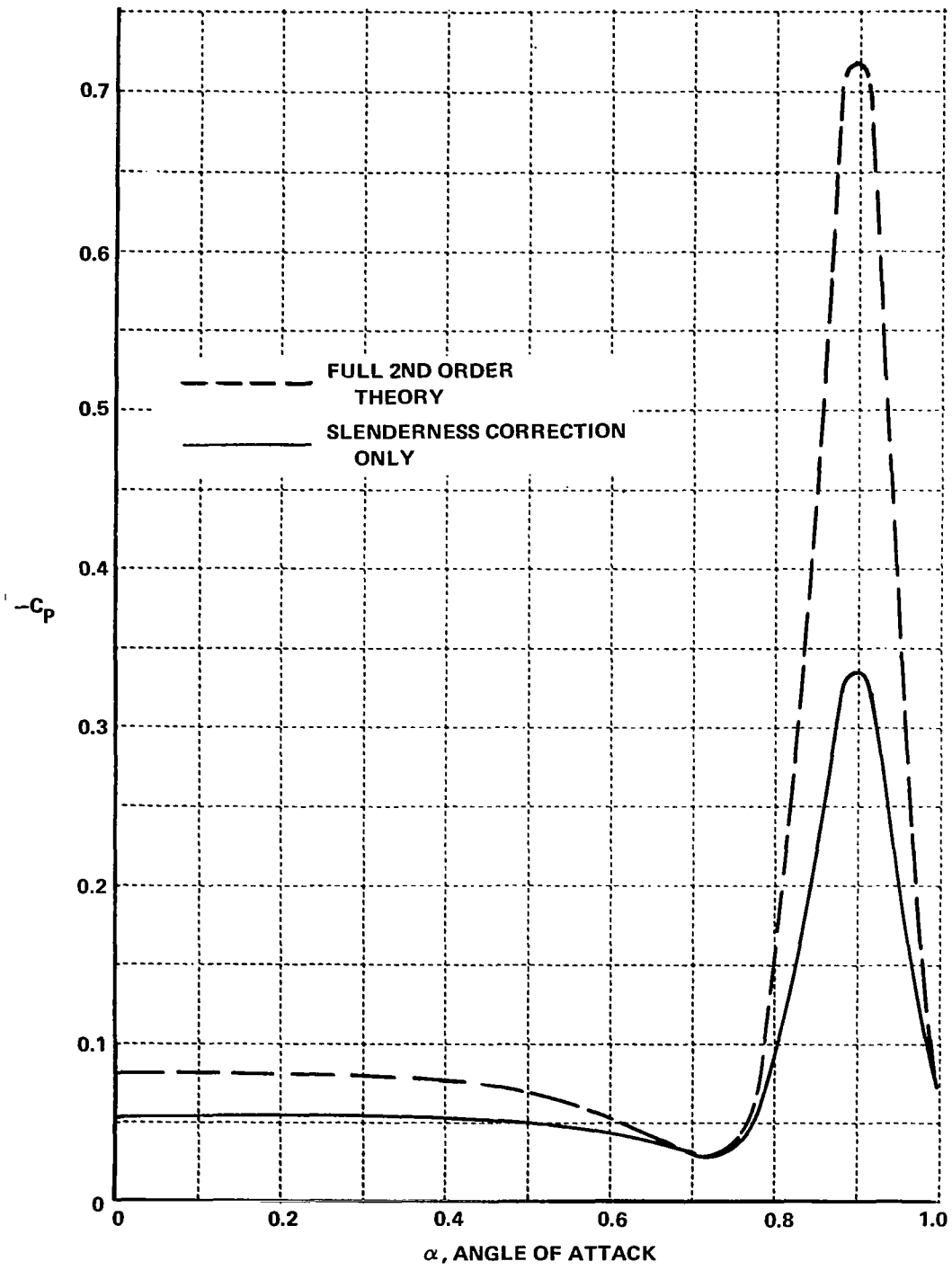

Figure 16 COMPARISON OF THEORETICALLY PREDICTED UPPER SURFACE PRESSURES, A = 1.0, α = 7.160, M = 3.3

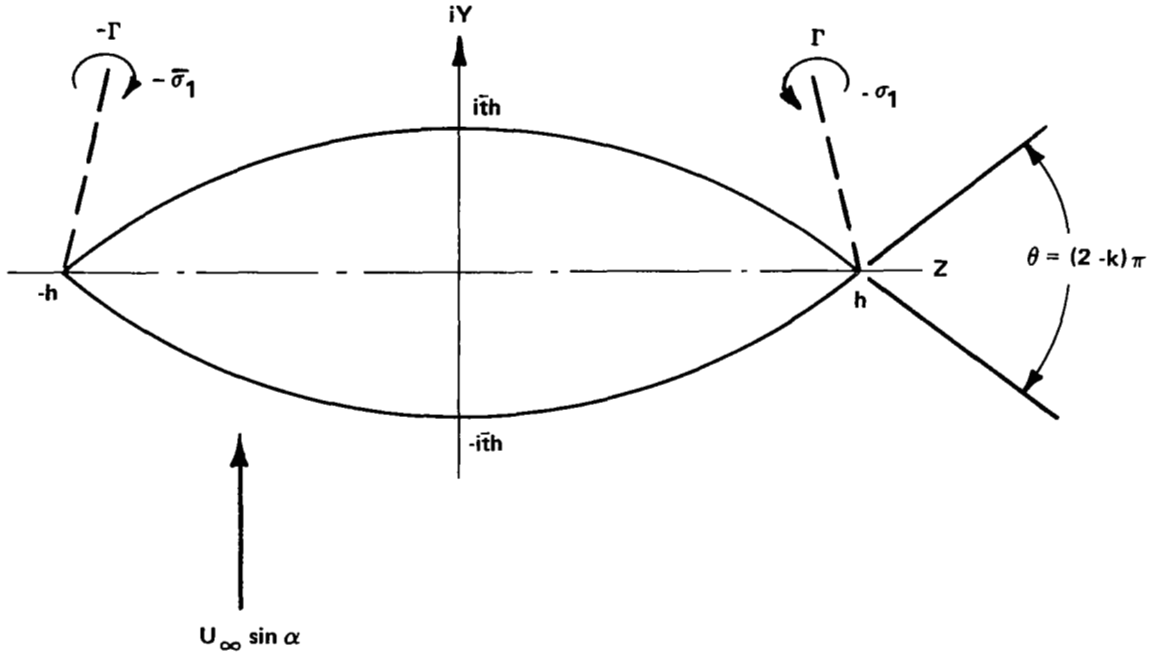

Figure 17A σ PLANE

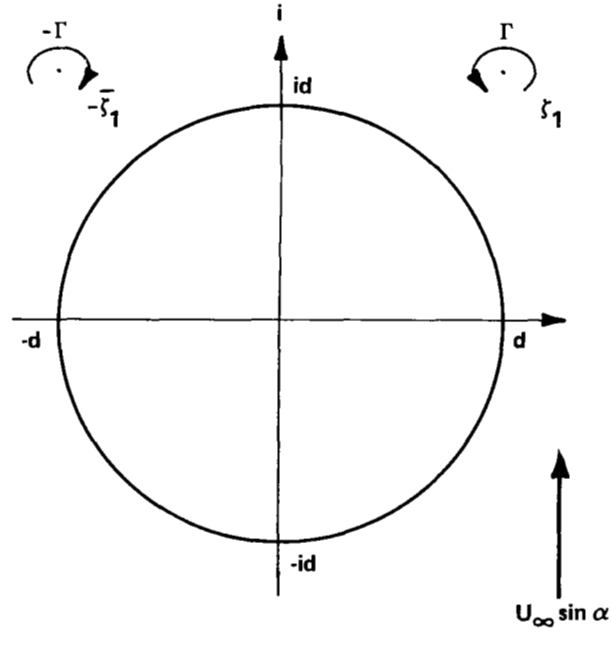

Figure 17B ζ PLANE

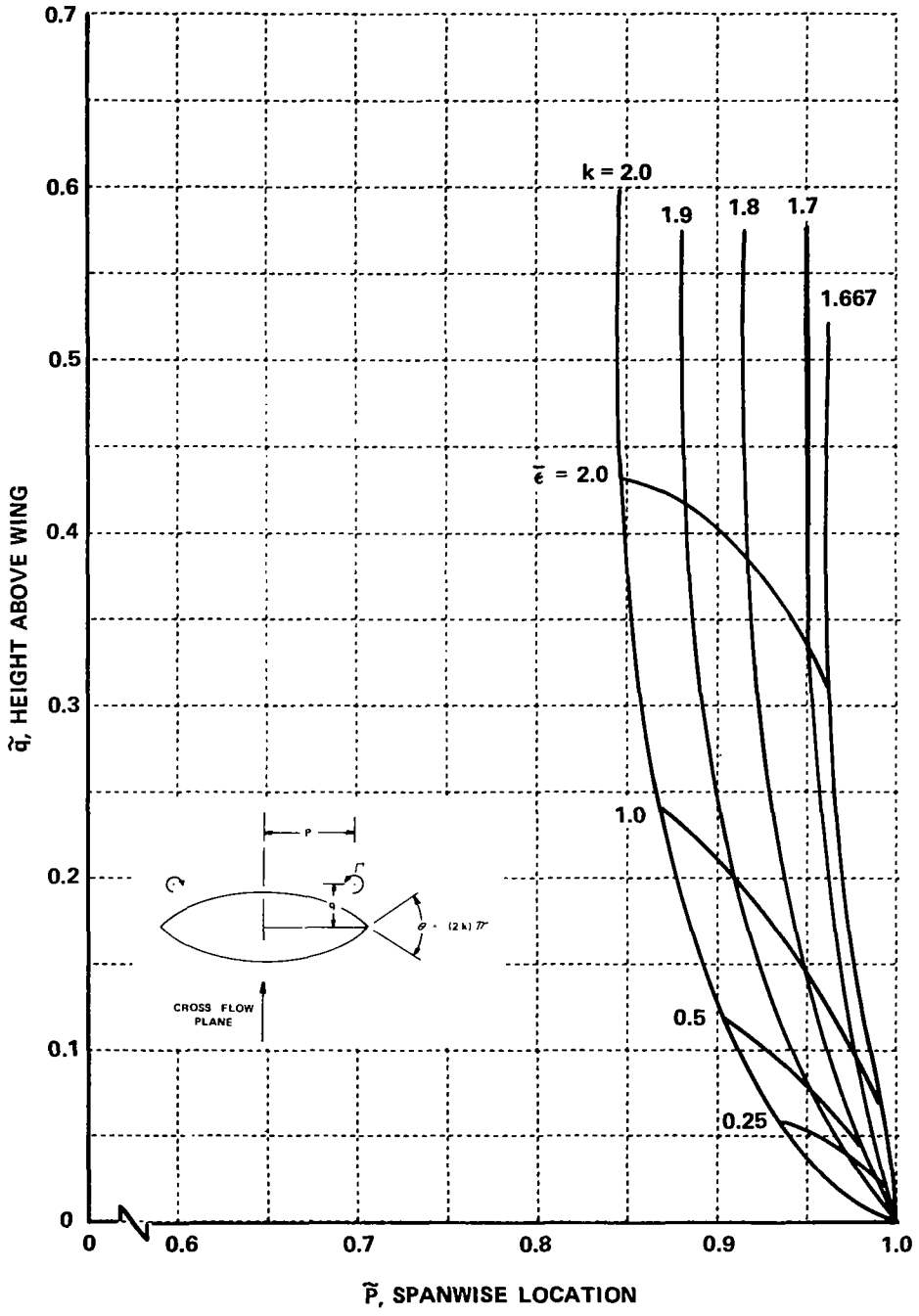

Figure 18 VORTEX POSITION FOR BICONVEX PROFILE DELTA WING

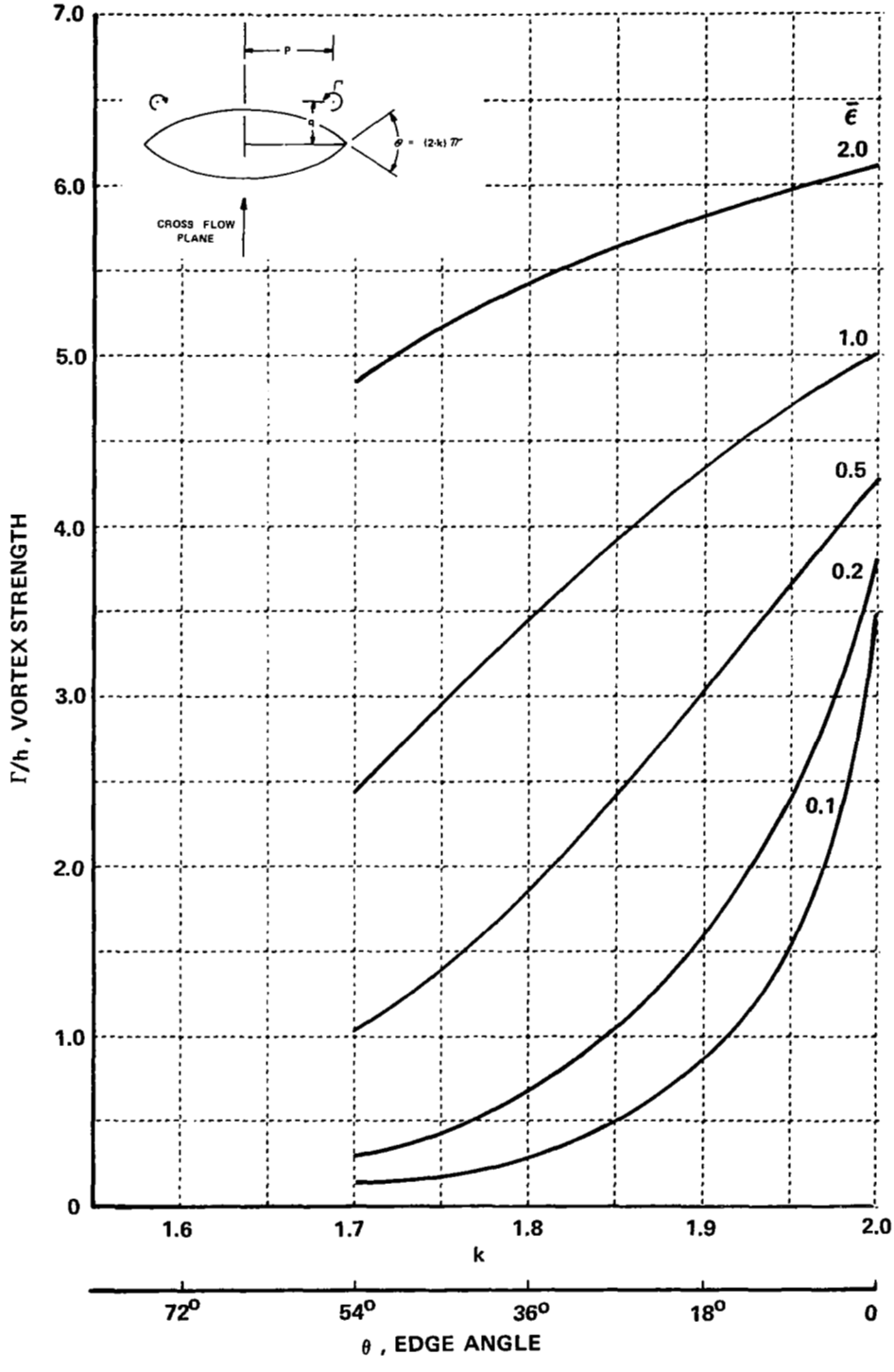

Figure 19 VORTEX STRENGTH FOR BICONVEX PROFILE DELTA WING

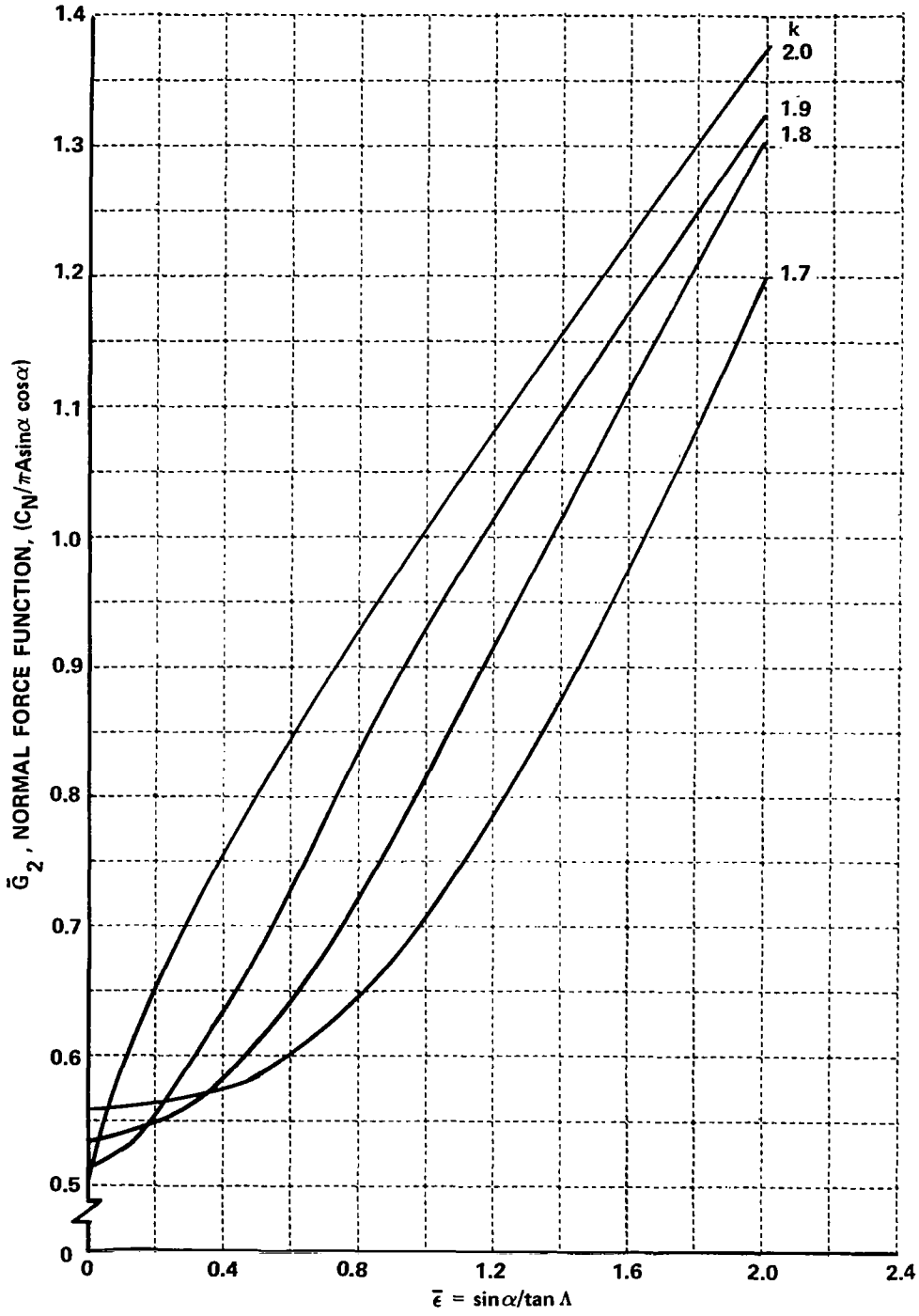

Figure 20 NORMAL FORCE FUNCTION FOR BICONVEX PROFILE DELTA WINGS

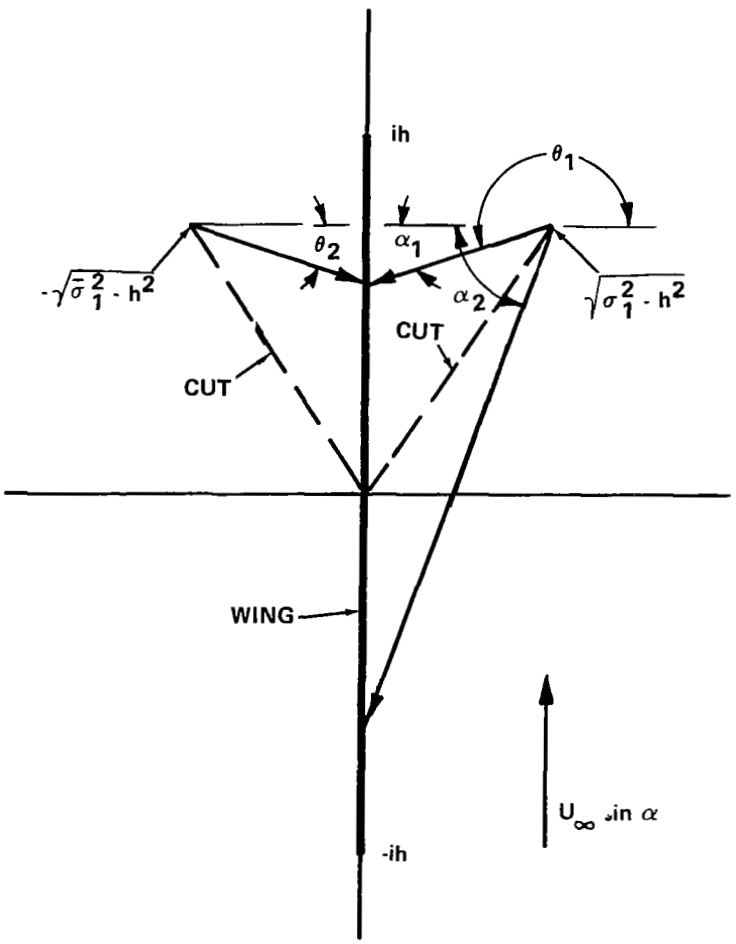

χ PLANE $\chi = \sqrt{\sigma^2 - h^2}$

Figure 21

NASA-Langley, 1971 —— 1 CR-1860